STRUCTURE OF THE DUNAMAGON GRANITE, BAIE VERTE PENINSULA, NEWFOUNDLAND

Laurel McDonald

Submitted in Partial Fulfilment of the Requirements
for the Degree of Bachelor of Science, Honours
Department of Earth Sciences
Dalhousie University, Halifax, Nova Scotia
March 1993

Dalhousie University

Department of Earth Sciences
Halifax, Nova Scotia
Canada B3H 3J5
(902) 494-2358
FAX (902) 494-6889

DATE April 26, 1993

AUTHOR Laurel McDonald

TITLE Structure of the Dunamagon Granite, Baie Verte Peninsula, Newfoundland

Degree BSc. Convocation May Year 1993

Permission is herewith granted to Dalhousie University to circulate and to have copied for non-commercial purposes, at its discretion, the above title upon the request of individuals or institutions.

Distribution License

DalSpace requires agreement to this non-exclusive distribution license before your item can appear on DalSpace.

NON-EXCLUSIVE DISTRIBUTION LICENSE

You (the author(s) or copyright owner) grant to Dalhousie University the non-exclusive right to reproduce and distribute your submission worldwide in any medium.

You agree that Dalhousie University may, without changing the content, reformat the submission for the purpose of preservation.

You also agree that Dalhousie University may keep more than one copy of this submission for purposes of security, back-up and preservation.

You agree that the submission is your original work, and that you have the right to grant the rights contained in this license. You also agree that your submission does not, to the best of your knowledge, infringe upon anyone's copyright.

If the submission contains material for which you do not hold copyright, you agree that you have obtained the unrestricted permission of the copyright owner to grant Dalhousie University the rights required by this license, and that such third-party owned material is clearly identified and acknowledged within the text or content of the submission.

If the submission is based upon work that has been sponsored or supported by an agency or organization other than Dalhousie University, you assert that you have fulfilled any right of review or other obligations required by such contract or agreement.

Dalhousie University will clearly identify your name(s) as the author(s) or owner(s) of the submission, and will not make any alteration to the content of the files that you have submitted.

If you have questions regarding this license please contact the repository manager at dalspace@dal.ca.

Grant the distribution license by signing and dating below.

_____ _____

Name of signatory Date

Abstract

New structural data from field observations and microstructural analysis are the basis of description of structures in the Dunamagon Granite, for the purpose of determining whether it has an intrusive, or tectonic, contact with adjacent rocks of the Humber and Dunnage Zones, and if the contact is tectonic, what type of structure it represents. Major tectonic structures in the Dunamagon Granite include an east-west striking foliation, oblique southeast-trending down-dip lineation, and east-west striking shear zones. The Dunamagon Granite intrudes the Pacquet Harbour Group to the south and is in tectonic contact with the Ming's Bight Group to the north. The northern boundary, along which the Dunamagon Granite and Pacquet Harbour Group were thrust, is interpreted as either a tectonically activated intrusive contact or as a purely tectonic contact between the Dunamagon Granite and the Ming's Bight Group. Depending on the interpretation, the Silurian age of the granite provides a maximum, or minimum, age of juxtaposition of the groups. Microstructural analysis revealed two generations (high and low temperature) of quartz microstructures in the Dunamagon Granite, probably formed by dislocation creep and grain boundary migration recrystallization during two deformation events. Mafic rocks in contact with the Dunamagon Granite preserve mineral assemblages representative of high (epidote-hornblende-biotite-quartz-plagioclase) and very low (prehnite) temperature metamorphism, suggesting two metamorphic events. The results of this study justify re-evaluation of the contact relations of the Dunamagon Granite and the timing of the juxtaposition of the Humber and Dunnage Zones in this area.

Key Words: Dunamagon Granite, Baie Verte Line, Ming's Bight Group, thrusting, microstructural analysis, deformation mechanisms

TABLE OF CONTENTS

TABLE OF FIGURES

TABLE OF TABLES

Acknowledgements

I would like to thank Dr. R.A. Jamieson, Dr. N. Culshaw, and Dr. D. B. Clarke for all their encouragement and assistance throughout this project. I also want to thank everyone who helped, especially S. Anderson for his patience in the field and for many discussions about my theis. Funding for this project was provided by Lithoprobe East.

CHAPTER 1 INTRODUCTION

"The Baie Verte Peninsula is unique within the Appalachian Orogen because the contact between the Paleozoic margin of North America and the ancient oceanic domain of Iapetus is nearly continuously exposed." -James Hibbard (1982)

1.1 Introduction and Regional Setting

Newfoundland is a geologically complex part of the northern Appalachians. Some of its geological history can be reconstructed by studying small, key localities. One such locality is the Baie Verte Peninsula, located in northwest-central Newfoundland and bounded to the east, west, and north by Notre Dame Bay, White Bay, and the Labrador Sea, respectively (Fig. 1.1).

Williams (1978) sub-divided the geology of Newfoundland into four tectonostratigraphic zones (from west to east: Humber, Dunnage, Gander, and Avalon) based on contrasts in the pre-Middle Ordovician geology. On the Baie Verte Peninsula, the Fleur de Lys Supergroup and the East Pond Metamorphic Suite represent continental margin rocks of the Humber Zone. The Dunnage Zone consists of ophiolite complexes, volcanic cover sequences, and intrusive rocks, represented on the Baie Verte Peninsula by, for example, the Point Rousse Complex, Pacquet Harbour Group, Flatwater Pond Group, Burlington Granodiorite, and the Dunamagon Granite. The Baie Verte Line (BVL), a narrow complex fault zone, and a major structural feature on the Baie Verte Peninsula, separates the Humber and Dunnage Zones and continues through the Appalachians as the Baie Verte-Brompton Line. The BVL represents an important part of the tectonic evolution of the Baie Verte Peninsula (Hibbard 1982).

On the Baie Verte Peninsula major geological structures, including the BVL, change from north-northeast to east-west trending. The Ming's Bight Group, generally included with the Fleur de Lys Supergroup, lies to the north of the easterly-trending part

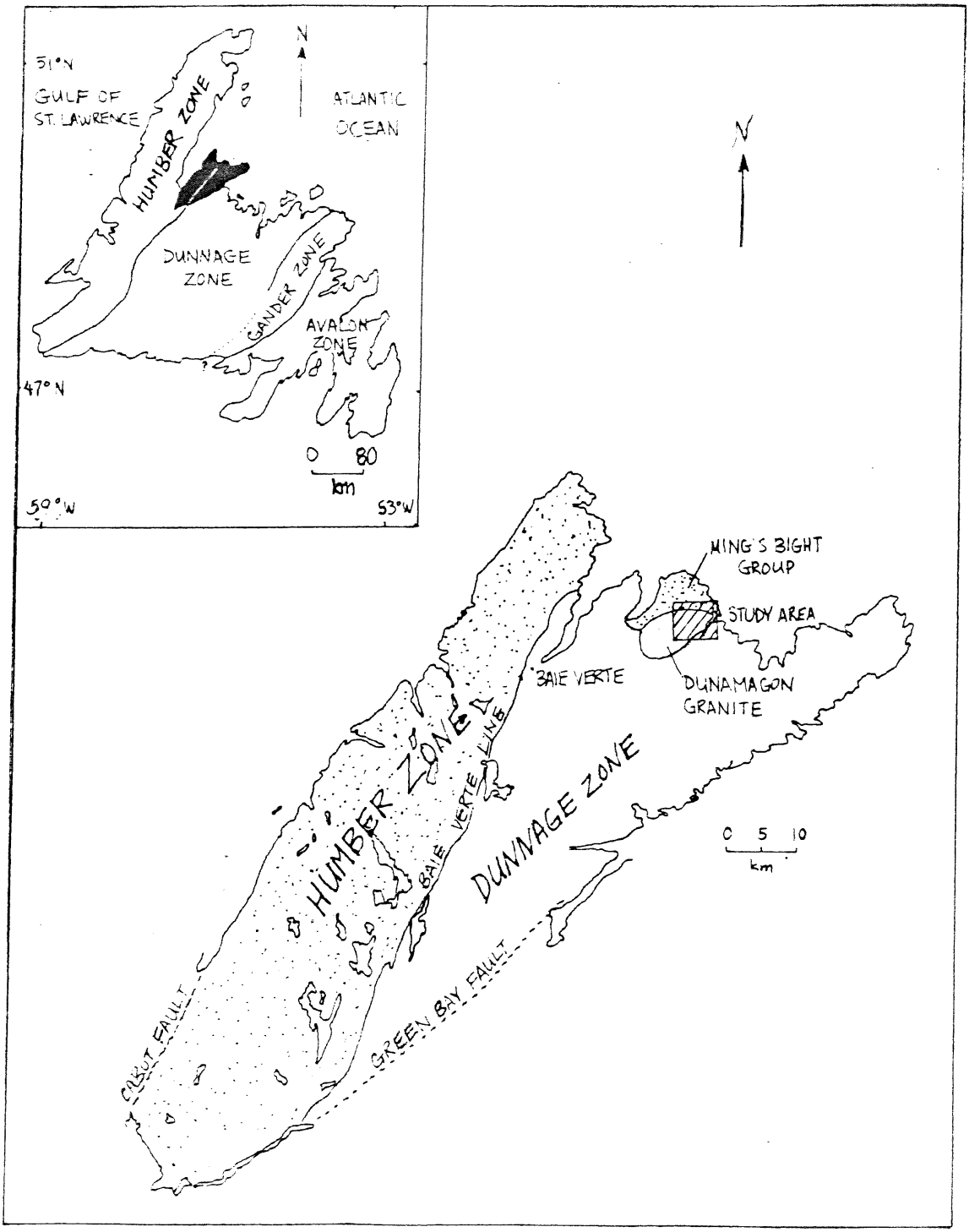

Figure 1.1 Map of the Baie Verte Peninsula (after Hibbard 1982 .), showing the study area. The stippled area represents rocks of the Humber Zone, including the Ming's Bight Group.

of the line. The isolation of the Ming's Bight Group from the main Fleur de Lys Supergroup and its location in the ophiolitic-volcanic terrane is a problem yet to be solved.

The Dunamagon Granite is also located on the easterly trending part of the BVL. This Silurian pluton (Dallmeyer and Hibbard 1984) crops out 15 km east of the town of Baie Verte (Fig. 1.1), and is in contact with the Ming's Bight Group to the north and the Pacquet Harbour Group to the south. Hibbard (1982), and Dallmeyer and Hibbard (1984), suggested that the Dunamagon Granite is a "stitching pluton" that intruded rocks on either side of the BVL, thus fixing a minimum age for movement along this tectonic boundary. This interpretation implies that the Ming's Bight Group and Pacquet Harbour Group were in contact prior to granite emplacement. The interrelation of the Dunamagon Granite, Ming's Bight Group, and Pacquet Harbour Group is thus crucial to understanding the sequence of events in this area. Tectonic structures in the Dunamagon Granite may help to reconstruct the deformation history of the pluton and the conditions of deformation.

1.2 Purpose

Establishing the relationship of the Dunamagon Granite to neighbouring groups is vital to understanding the tectonic events and their timing on the Baie Verte Peninsula. The main objectives of this study are:

- to describe structures within the Dunamagon Granite based on field observations and microstructural analysis; and
- to determine whether the Dunamagon Granite has an intrusive, or a tectonic, contact with adjacent rocks, and if the contact is tectonic, what type of structure does it represent?

This problem is significant in terms of understanding the timing of the juxtaposition of the Humber and Dunnage Zones in this area and the timing of any movement along this portion of the Baie Verte Line.

1.3 Scope

The focus of this thesis is structural geology. Exposure and accessibility limit the geographic scope of this study to the eastern portion of the pluton, with the emphasis of field work on the northern contact of the Dunamagon Granite with the Ming's Bight Group. The geochemical part of this investigation consists only of electron microprobe analysis for the purpose of estimating P-T conditions; however this thesis makes no attempt to model a P-T-t path for the Dunamagon Granite. Although dating the Dunamagon Granite is not part of this thesis, the structural results will help other workers interpret the geochronology of the granite.

1.4 Methods

Field work involved mapping structures along the contacts of, and within, the Dunamagon Granite through traverses across the granite, brook traverses, and detailed mapping of coastal exposure. Mapping was undertaken at 1:12 500 using aerial photographs, accompanied by field notes with detailed descriptions of individual locations. Samples, accurately oriented if possible, were collected wherever significant change in the orientation or nature of structures occurred, and at sufficient intervals to fully describe the tectonic structures present in the granite. Field observations and microstructural analyses of oriented thin sections provide the basis for structural descriptions. Electron microprobe analysis of textures, structures, and mineral compositions was performed on a small number of samples. Estimation of general P-T conditions of deformation utilizes microstructures and mineral assemblages.

1.5 Organization

This thesis first familiarizes the reader with the geology of the Baie Verte Peninsula, and with some of the complications of the regional tectonics. Descriptions of

the local geology focus on the main groups involved in this study (Ming's Bight Group, Dunamagon Granite, Pacquet Harbour Group). A discussion of field observations of structures within the Dunamagon Granite and its contact relations follows. A comparison of microstructural evidence with macro- and meso-structural evidence supports field-based interpretations. The concluding chapter summarizes the regional significance of this study considered in a regional context.

CHAPTER 2 FIELD RELATIONS

2.1 Previous Work

The Ming's Bight Group, Pacquet Harbour Group, Peleé Point Schist, and Dunamagon Granite have been studied by Baird (1951), Neale (1958), Church (1969), Kennedy (1975), DeGrace et al (1976), and many others, including more recent work by Hibbard (1983) (Fig. 2.1). An extensive study of the area by S. Anderson is now in progress (MSc project, Dalhousie University). With two exceptions, the results of the present study are similar to the findings of previous studies. First, earlier workers believed that the Dunamagon Granite intruded both Ming's Bight Group and the Pacquet Harbour Group. Baird (1951) attributed pegmatites in the Ming's Bight Group to the intrusion of the Dunamagon Granite , and DeGrace et al (1976) reported xenoliths of Ming's Bight Group psammite within the Dunamagon Granite. However, results of this study suggest that this contact is tectonic. Second, most workers (Neale 1958; Church 1969; Kennedy 1975; DeGrace et al 1976; and Williams et al 1977) associated the Pelée Point Schist, a controversial informal unit described in Section 2.4, with the Pacquet Harbour Group. They therefore considered the contact between the Ming's Bight Group and the Pelée Point Schist to be the conformable contact of the Ming's Bight Group and Pacquet Harbour Group. However, Hibbard (1983) included the Pelée Point Schist at Pelée Point as a conformable member of the Ming's Bight Group. Evidence from this study supports inclusion of the Pelée Point Schist with the Pacquet Harbour Group, but suggests that the Ming's Bight Group - Pacquet Harbour Group contact is tectonic. This chapter addresses these two issues.

2.2 Ming's Bight Group

The Ming's Bight Group consists of medium- to coarse-grained, buff- to grey-coloured psammite, semi-pelitic schist, and metaclastic rocks. Psammite is the dominant

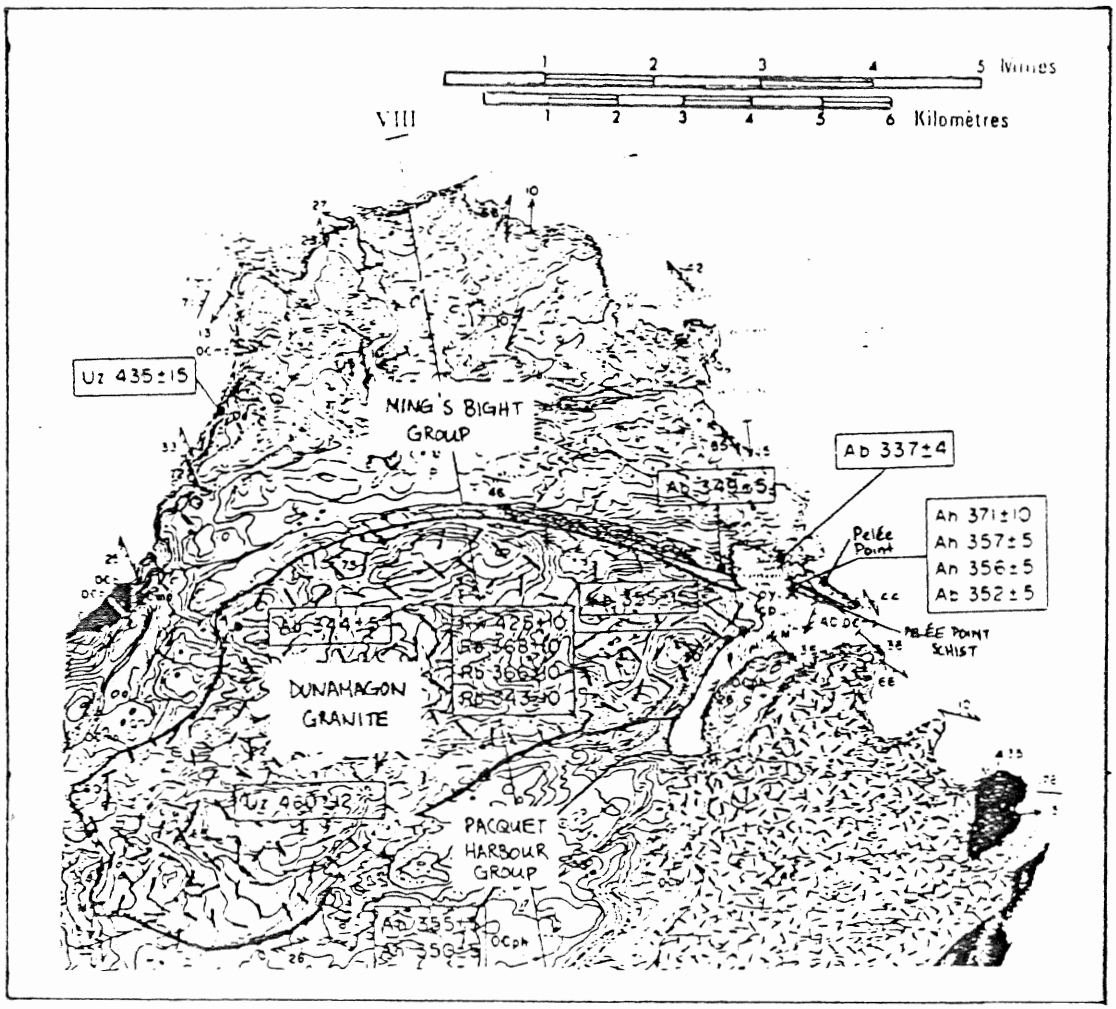

Figure 2.1 Map of the study area after Hibbard (1983), showing the Ming's Bight Group, Dunamagon Granite, Pacquet Harbour Group, and Pelée Point Schist. This study concentrates on the Dunamagon Granite and its contacts, especially with the Ming's Bight Group. Note the location of Pelée Point. The numbers represent argon dates.

lithology and consists of quartz, feldspar, white mica, biotite, and rare garnet. The semi-pelitic schist contains biotite- and white mica-rich layers. In the Big Brook Shear Zone, a 500m wide and 4 km long zone in the southern Ming's Bight Group, large, randomly-oriented flakes of white mica occur in the schist. In one area pelite containing idioblastic staurolite porphyroblasts (Fig. 2.2) surrounds kyanite-bearing quartz pods. Pods of actinolite schist occur along the contact between the Pelée Point Schist and the Ming's Bight Group. Associated with the Pelée Point Schist on the west side of the group are pods of talc-carbonate, actinolite-carbonate schist, metagabbro-like rock, and actinolite-biotite rock (Hibbard 1983). The general strike of structures (fold axial planes, foliation) in the Group is east-west, but dips are highly variable. The Group is polydeformed and metamorphosed to greenschist, and locally amphibolite, grade. Locally preserved primary structures suggest that the Ming's Bight Group represents a turbidite sequence. A full Bouma sequence is not preserved, but the turbidite sequences are recognizable on the basis of distinct boundaries, fining-upwards sequences, and the cyclic nature of these sequences at outcrop scale. Deformed and undeformed pegmatites of uncertain origin cut the Ming's Bight Group.

2.3 Pacquet Harbour Group

2.3.1 Pacquet Harbour Group

Hibbard (1983) describes the Pacquet Harbour Group as a moderately to steeply northerly dipping sequence of variably deformed and metamorphosed mafic volcanic and volcaniclastic rocks, felsic volcanic rocks, and mafic dykes. In the north the Pacquet Harbour Group is polydeformed and polymetamorphosed. The rocks are of lower amphibolite facies and display multiple fabrics. Farther south the rocks are of greenschist grade and have only one fabric. Pillow lavas of the Pacquet Harbour Group, which consist mainly of actinolite, albite, and epidote, with minor chlorite and quartz, may represent the top of an ophiolite sequence.

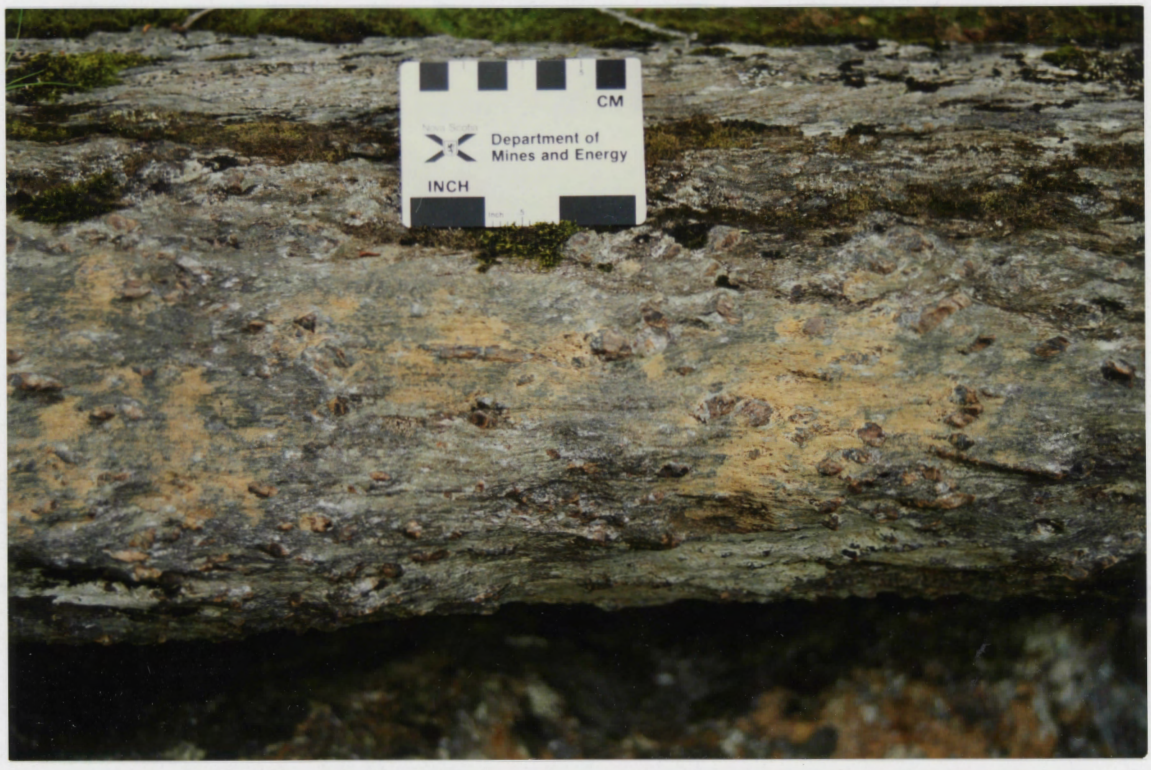

Figure 2.2 Staurolite schist in the Big Brook Shear Zone (Station 41). This is not typical of the entire Big Brook Shear Zone. At this location both kyanite and staurolite are present.

Mafic volcaniclastic and epiclastic rocks are thickly bedded, reworked, green tuff with minor chert, and a crystal tuff that serves as a marker horizon. However, most of the Pacquet Harbour Group remains undivided. Mafic intrusive rocks associated with the Pacquet Harbour Group range in texture from coarse pegmatite to fine-grained diabase (Hibbard 1983). In the north, near the contact with the Dunamagon Granite, the Pacquet Harbour Group is fine-grained, green-grey, foliated mafic rock containing small white feldspar crystals, with thin bands of plagioclase throughout.

2.3.2 Pelée Point Schist

This unit includes greenschist and amphibolite that crops out with the Ming's Bight Group in four areas. According to Hibbard (1983), the schist in the Ming's Bight area is composed of foliated, fine- to medium-grained actinolite-chlorite-albite schists, satiny chlorite pelite, and gritty chloritic metasediments. On Pelée Point (Fig. 2.3), the schist, which is of higher metamorphic grade than elsewhere, is a fine-grained, blackish green, hornblende-biotite-plagioclase rock. The hornblende porphyroblasts contained within the plane of the foliation show strong lineation in some areas, and random orientations in other areas. The porphyroblasts range in size from a few millimetres to over 1.5 centimetres long. Locally, feldspar porphyroblastic layers contain crystals 2-7 cm long. A section of pillow lava exposed along the southern coast of Pelée Point is part of the Pelée Point Schist.

The lithology of the Pelée Point Schist at Pelée Point is essentially identical to that of the Pacquet Harbour Group on the eastern side of Pacquet Harbour. The presence of a sheared contact with the Ming's Bight Group, and the higher metamorphic grade of the Peleé Point Schist with respect to the adjacent psammites, suggests that it is not conformable with the Ming's Bight Group. On

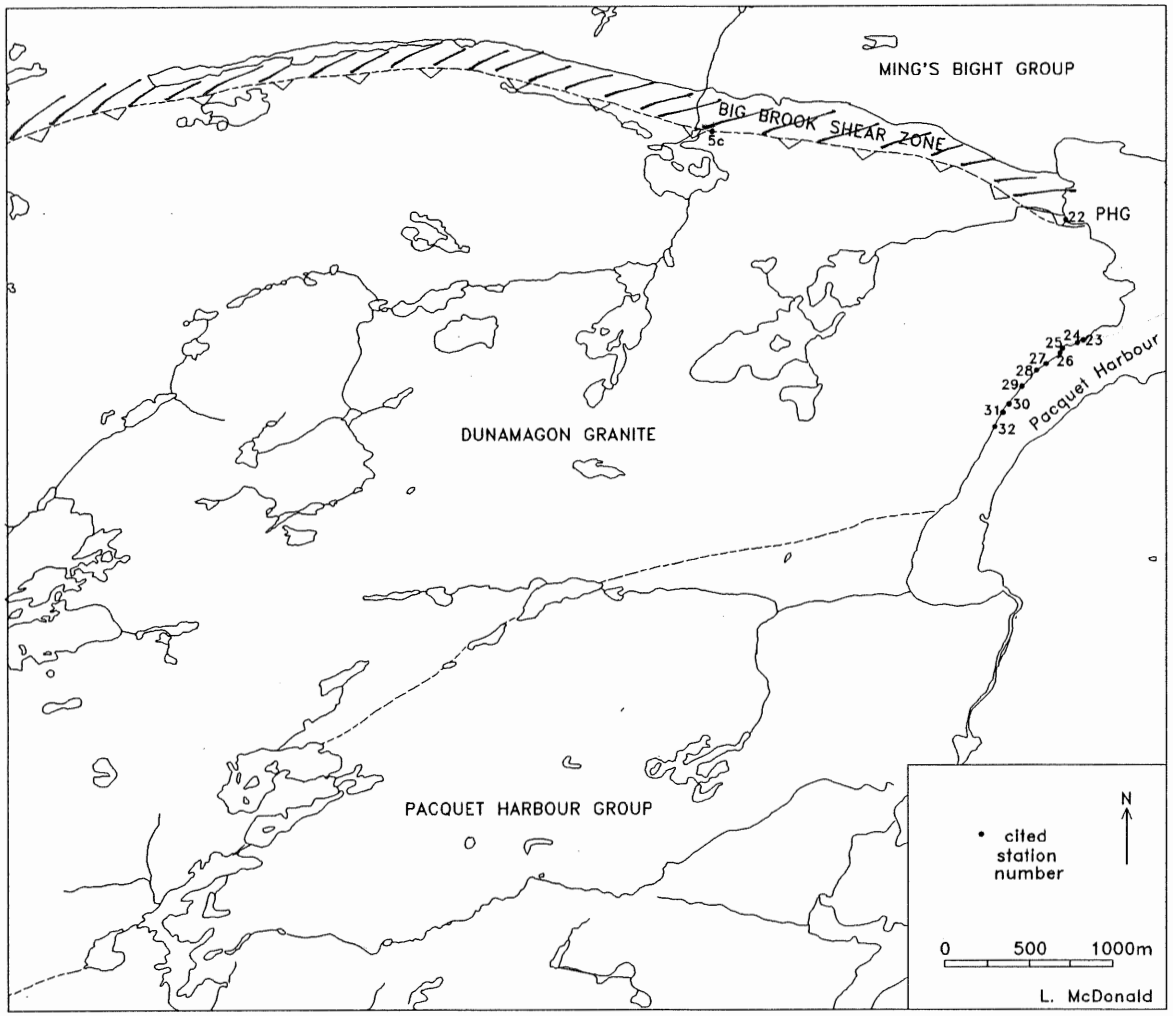

Figure 2.3 Geological map of the Study area showing the Ming's Bight Group, Dunamagon Granite, Pacquet Harbour Group, and Big Brook Shear Zone, with numbers of stations cited in the text.

the basis of this evidence, the Peleé Point Schist is considered to be part of the Pacquet Harbour Group.

2.4 Contact between the Ming's Bight Group and Pacquet Harbour Group

The contact of the Ming's Bight Group with the Pelée Point Schist is, by definition, the contact with the Pacquet Harbour Group. On Pelée Point the contact is marked by an approximately 1 m wide zone of rust-coloured schist that is part of a shear zone (Fig. 2.4). The Ming's Bight Group semi-pelite to the north of this easterly-striking shear zone contains garnet and biotite of greenschist grade. To the south of the shear zone, the Pelée Point Schist contains abundant amphibole, but garnets and biotite are absent. This abrupt mineralogical change, corresponding to differences in metamorphic grade, and the intensely deformation of the shear zone strongly suggests that these two groups are in tectonic contact. At Station 22 folded psammite of the Ming's Bight Group is in contact with mylonite of Pacquet Harbour Group material, which is also folded. This structural evidence also supports a tectonic contact between these two groups.

2.5 Dunamagon Granite

The Dunamagon Granite is a pink, fine- to medium-grained biotite granite. One of several Silurian plutons on the Baie Verte Peninsula (Dunning and Cawood, submitted), the Dunamagon Granite is approximately 10 km long and 4 km wide at its maximum dimensions. The granite is not uniform in texture or composition (Baird 1951). Deformation of the granite resulted in two sets of inhomogeneously developed structures. The fabrics, defined by the orientation of biotite and the elongation of feldspar, vary in intensity and orientation throughout the pluton. In fact, in the south some areas of the granite are undeformed, with igneous, rather than metamorphic, texture. The general composition of the granite is 30-40% quartz, 40-50% feldspar, and 5-15% biotite. K-feldspar and plagioclase occur in the groundmass and K-feldspar as phenocrysts. Some of

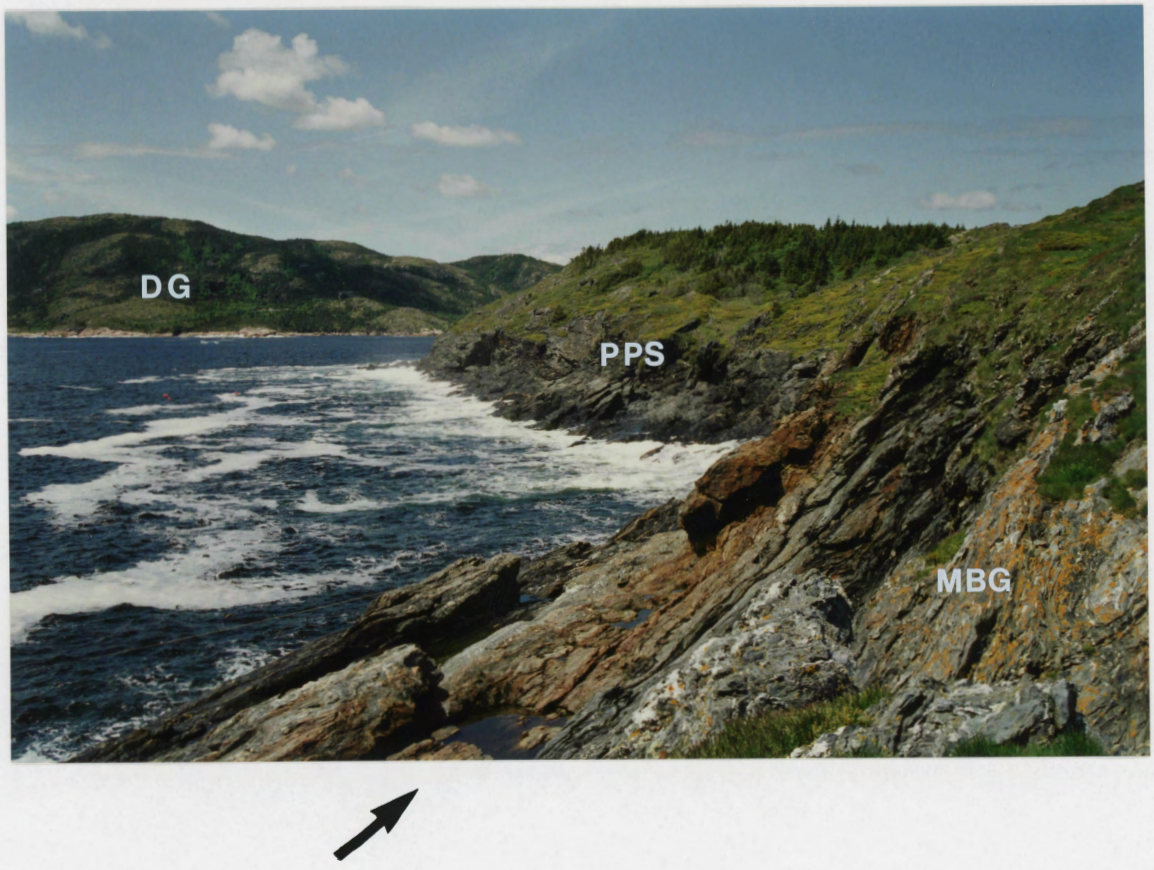

Figure 2.4 The contact of the Pelée Point Schist with the Ming's Bight Group (marked by the arrow). This photograph was taken on Pelée Point, facing west, looking along strike of the units. The green-grey unit on the right is the Ming's Bight Group. The rusty zone is the contact of the Ming's Bight and Pelée Point Schist (black unit in the centre of the photgraph). The pink exposed rock in the background and the hills in the left of the photograph is Dunamagon Granite.

the K-feldspar phenocrysts show evidence of rotation but they are equivocal as to the direction of rotation because they are not strongly asymmetric; only locally do they serve as mesoscopic shear sense indicators.

2.6 Contact Relations

The Big Brook Shear Zone defines the northern boundary of the Dunamagon Granite, and its contact with the Ming's Bight Group. The contact of the Dunamagon Granite and Ming's Bight Group is exposed in a small brook at Station 5c. At the contact, the granite is sheared and the Ming's Bight Group semi-pelitic schist shows no evidence of contact metamorphism. Granitic dykes are not present in the Ming's Bight Group, but pegmatites may be related to the Dunamagon Granite. DeGrace et al (1976) reported Ming's Bight Group xenoliths in the Dunamagon Granite, however this was not confirmed during this study.

The contact of the Dunamagon Granite with the Pacquet Harbour Group to the south is poorly exposed, however there are granitic dykes resembling Dunamagon Granite within the Pacquet Harbour Group to the north (Pelée Point Schist) and within the main Pacquet Harbour Group. Mafic xenoliths occur within the pluton. The evidence suggests an intrusive contact with the Pacquet Harbour Group.

2.7 Summary

The Dunamagon Granite intrudes the Pacquet Harbour Group and has a tectonic contact with the Ming's Bight Group along the Big Brook Shear Zone. The Pelée Point Schist is defined as part of the Pacquet Harbour Group; therefore, the sheared, tectonic contact between the Pelée Point Schist and Ming's Bight Group is the contact of the Ming's Bight Group with the Pacquet Harbour Group. Structures in the granite described in the following chapters form the basis for possible interpretations of these results proposed in Chapter 6.

CHAPTER 3 MACRO- AND MESOSTRUCTURES OF THE DUNAMAGON GRANITE

3.1 Introduction

The Dunamagon Granite is pervasively and heterogeneously deformed. A tectonic foliation developed in the granite varies in orientation and intensity across the pluton, and constrains the structure of its northern boundary. In addition to tectonic fabrics (foliation, lineation, shear zones), aplite dykes, quartz veins, and mafic bodies occur within the granite. This chapter describes the nature, and relative age, of macro- and mesostructures of the Dunamagon Granite.

3.2 Foliation

Aggregates of biotite and deformed K-feldspar, plagioclase, and quartz define a pervasive foliation within the Dunamagon Granite (Fig. 3.1). In most areas the foliation is sinuous, consisting of biotite wrapping around K-feldspar porphyroclasts, and planar foliation is well-developed in shear zones. Recrystallization of feldspar and reduction of grain size occurs in the shear zones. These foliations, throughout the pluton, generally strike east and dip gently to moderately southward (Fig. 3.2, Fig. 3.3).

3.3 Lineation

Mineral lineations in the Dunamagon Granite are generally weak or absent, but developed best in the north and in wide shear zones. The alignment of biotite edges and elongation of deformed feldspar define the lineation (Fig. 3.4). The lineation trends predominantly to the southeast, plunging moderately (18-45°) (Fig. 3.5) obliquely down dip on the foliation surfaces.

Figure 3.1 Vertical section of the typical Dunamagon Granite foliation (Station 11A) with biotite wrapping around K-spar porphyroclasts (foliation 068/25).

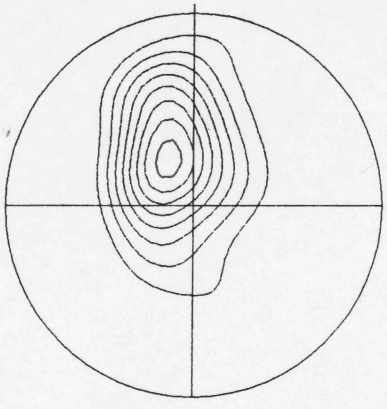

peak position: 333.4 / 69.8

Figure 3.2 This plot of poles to the foliation in the Dunamagon Granite (71 points) shows that the foliation is gently to moderately dipping and east-west striking. The lowest contour level represents a density of 4 points and the contour interval is 2.66 (2σ).

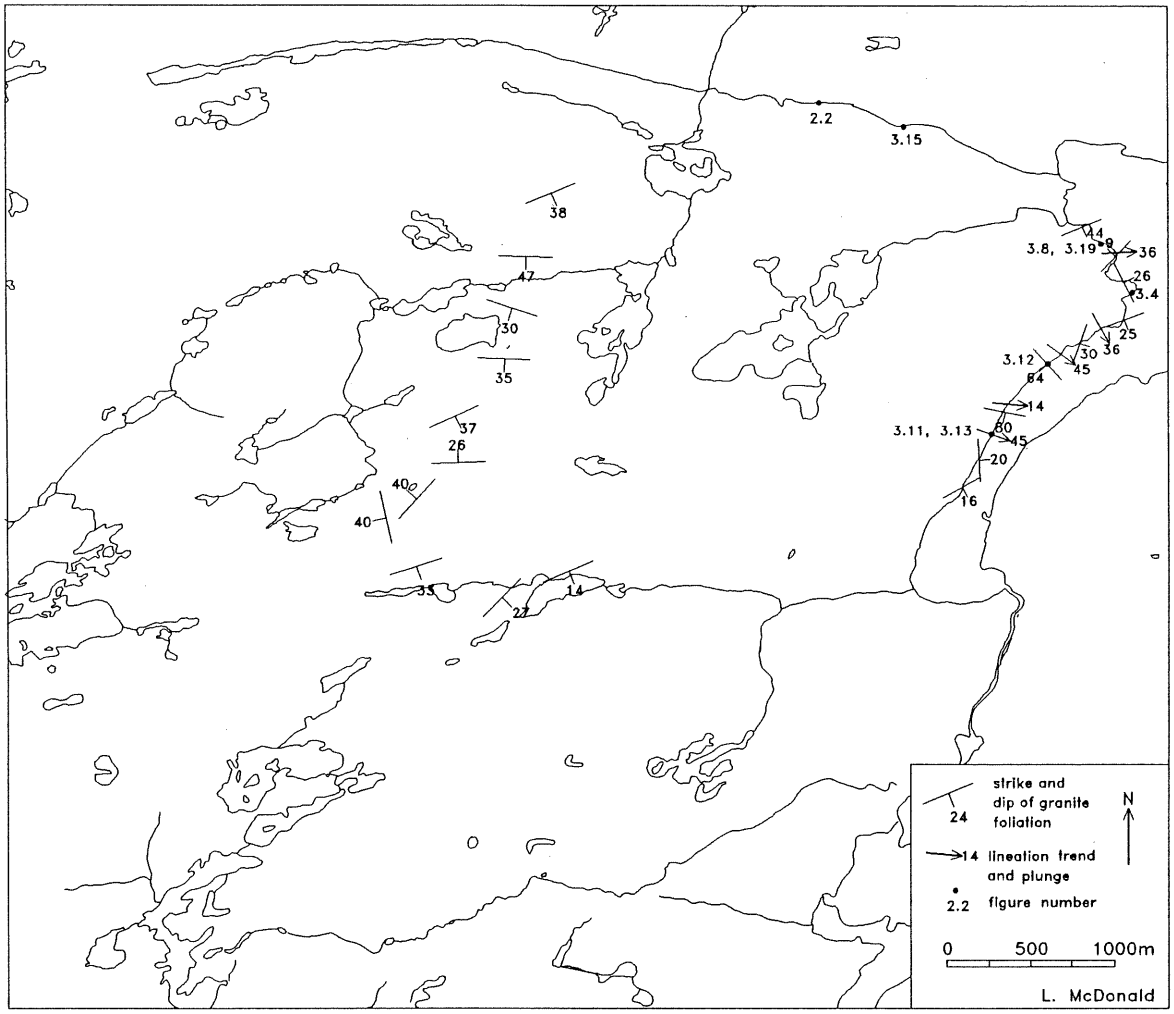

Figure 3.3 Foliations and lineations in the Dunamagon Granite. The numbers represent photograph locations.

Figure 3.4 Well-deveolped Dunamagon Granite lineation on a foliation surface (Station 13). The pencil parallels the lineation and points down plunge.

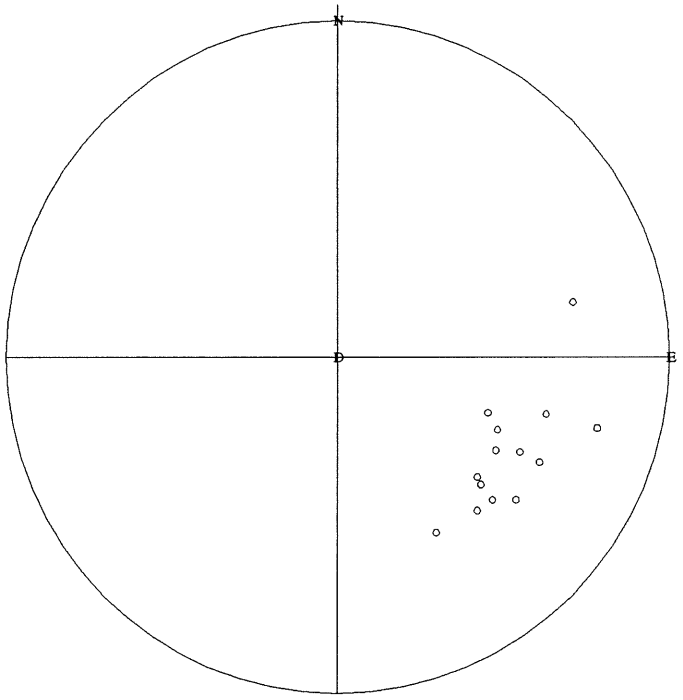

Figure 3.5 Mineral lineations in the Dunamagon Granite (9 points), predominantly southeast trending, moderately plunging, oblique to the foliation.

3.4 Aplite Dykes

Aplite dykes are an early feature in the Dunamagon Granite because they do not cross-cut the earliest foliation. The dykes range in size from 10-75 cm wide, and from three to tens of metres long. The dykes show pervasive deformation, and are cut by later structures, for example quartz veins and shear zones (Fig. 3.6). At Station 24, an aplite dyke has a horizontal separation of 9 m along a shear zone (246/83) and at Station 16, a foliation developed in an aplite dyke is parallel to the foliation in the surrounding granite. On a stereogram plot (Fig. 3.7) the poles to the aplite dykes lie on a great circle, the pole of which is sub-parallel to the granite lineation. This suggests that the aplites may have an intersection lineation related to the deformation of the granite.

3.5 Quartz Veins

Quartz veins are ubiquitous within the Dunamagon Granite. Their orientations varies somewhat (Fig. 3.8) but they predominantly strike NNW to ENE, and are moderately (32-60°) to steeply dipping (63-77°) The veins range in size from 5-20 cm wide by 2-10 m long, and many are *en echelon*. Several generations of veins are present, all post-dating the aplite dykes, some veins which are cut by narrow shear zones, and some of which cut narrow shear zones.

3.6 Mafic Bodies

Mafic bodies are present along the coastal exposure of the Dunamagon Granite (Fig. 3.9). These tabular bodies are typically 1 m wide, and at least 10 m long because they are longer than the outcrops. The bodies are fine-grained, greenish-black in colour, and locally contain randomly-oriented, cream-coloured, tabular feldspar porphyroblasts (0.2-1.0 cm wide by 0.5-2.0 cm long) in amphibolite matrix. Their average composition is 45% biotite, 20% amphibole, 35% feldspar. An early fabric (S_1) in the mafic bodies is

Figure 3.6 Apparent cross-cutting relations of an aplite dyke (017/30), quartz vein (202/74), and mafic body (078/76) (Station 20). The aplite dyke is not actually in contact with the mafic body (see location of arrow).

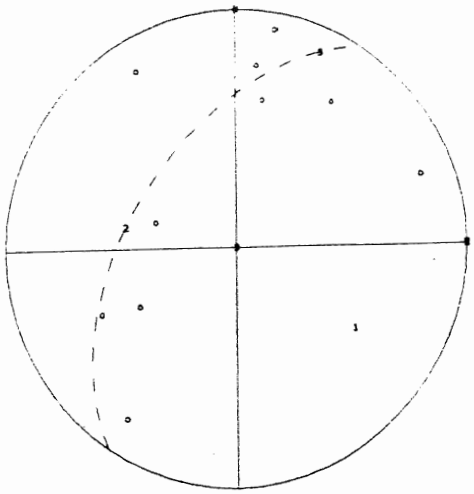

Figure 3.7 Poles to aplite dykes (10 points) weakly defining a great circle (dashed line). The line represents the best-fit great circle for the data, and is normally used to determine whether structures are folded, but there is not enough data for the Dunamagon Granite to conclude this about the dykes.

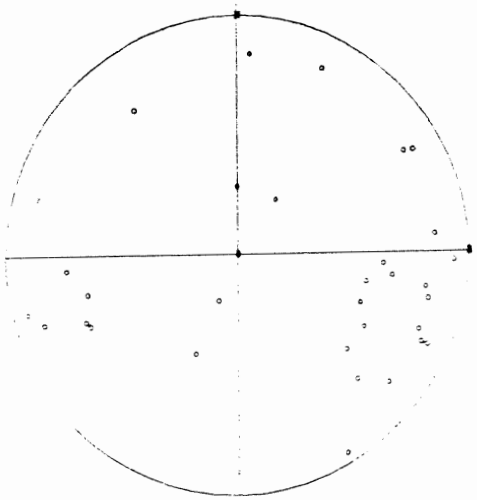

Figure 3.8 Poles to quartz veins showing a wide variety of orientations, but with clusters of steeply dipping veins (31 points)

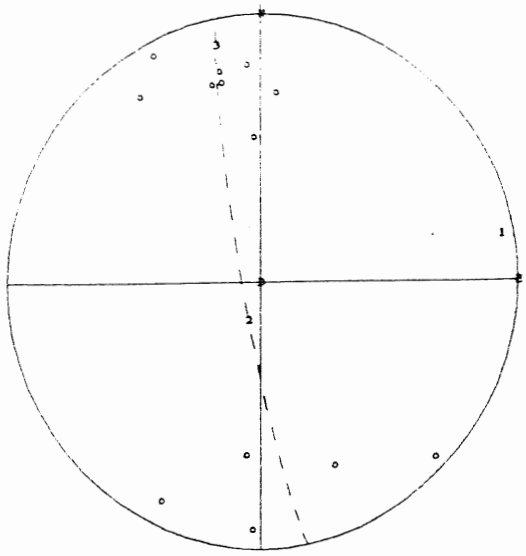

Figure 3.9 Poles to mafic bodies (13 points) showing that the steeply dipping bodies strike east-west.

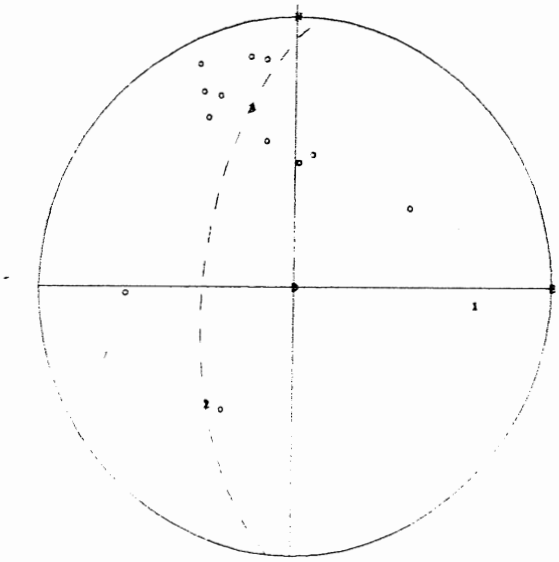

Figure 3.10 Poles to the crenulation in the mafic bodies (12 points) showing that the crenulation is moderate to steeply dipping and approximately east-west striking. The cluster of poles in the upper left quadrant is similar to the orientation of the mafic bodies (above).

crenulated. This crenulation, which parallels the foliation in the granite, is the dominant foliation in the mafic bodies (Fig. 3.10).

The origin of these bodies, as xenoliths or dykes, is uncertain. No cross-cutting relations exist among the quartz veins, aplite dykes, and mafic bodies. Recrystallization of the bodies obscures any evidence of a chilled margin, and preferential erosion of the mafic material along the coast makes observation difficult. Known mafic xenoliths are pale green-grey, highly assimilated, and rounded. However, the bodies show no evidence of assimilation at the contact with the granite. Field evidence is inconclusive, but possible interpretations are proposed in Chapter 6.

3.7 Shear Zones

Two morphologically distinct types of shear zones occur within the Dunamagon Granite. The following sections summarize the characteristics of each type.

3.7.1 "Wide" Shear Zones

Wide shear zones in the Dunamagon Granite range from 0.75-1.25 m in width and extend for a minimum of tens of metres in length to a maximum of 125 m (larger than outcrop scale). Within these zones feldspar crystals are uniformly fine and equigranular, augen are absent as a result of recrystallization, quartz is segregated into thin layers, and grain size is reduced compared to granite outside the shear zones. The sheared granite often appears darker than the surrounding granite. Figure 3.11 shows a shear zone with a tension gash that indicates an apparent dextral sense of shear observed in the horizontal plane (foliation 094/77, lineation 110→45). At Station 32, a similar gneissic shear zone with a well-developed planar foliation lacks macroscopic shear-sense indicators. Apparent sinistral shearing, observed in the horizontal plane, within a single shear zone is

Figure 3.11 Wide shear zone at Station 33 (foliation 094/77, lineation 110→45). Note the decreased grain size and strong foliation (viewed in horizontal plane). The tension gash (341/77) indicates apparent dextral shearing. The top of the photo is north.

continuous through Stations 24, 25, 26, with the greatest apparent displacement (9m) occurring at Station 24.

3.7.2 "Narrow" Shear Zones

The narrow shear zones are 1 cm in width, dark, fine-grained bands that are typically a few metres in length. These narrow shear zones are parallel to each other and occur in clusters or in zones up to 12 m wide (Fig. 3.12). These zones are distinct from wide shear zones because shearing is discontinuous, rather than continuous across the zone. Separations of quartz veins and aplite dykes along these shear zones are usually not more than a few centimetres, although an aplite dyke displays a sinistral separation of 50 cm along a narrow shear zone at Station 23 (Fig. 3.13). Whereas the separation in the horizontal plane along a single narrow shear zone is small, on the order of a few (5-10) centimetres, the sum for these shear zones may represent significant displacement (>2 m). The narrow shear zones never cut the wide shear zones, or *vice versa*, and their orientations are similar (Fig. 3.14). At Stations 19, 23, 25, and 28 separation of dykes and veins along these narrow shear zones is sinistral and at Stations 27, 29, 30, 31 separation is dextral.

3.8 Big Brook Shear Zone

This shear zone occurs mainly within the Ming's Bight Group, but defines much of the northern boundary of the Dunamagon Granite. Rocks in the Big Brook Shear Zone (BBSZ) are strongly foliated (Figs. 3.15, 3.16) and have a well-developed lineation (Fig. 3.16). The foliation in the BBSZ and fold axial planes in the Ming's Bight Group (Fig. 3.17) are parallel to aplite dykes and mafic bodies in the Dunamagon Granite. The lineation in the shear zone and hinge lines in the Ming's Bight Group (Fig. 3.18) are parallel to the lineation in the Dunamagon Granite and the intersection lineation of the

Figure 3.12 Set of narrow shear zones at Station 27. The thin black lines are shear zones. Note the dextral separation of the aplite dyke (marked by arrow on left) and sinistral separation of quartz vein (marked by arrow on right).

Figure 3.13 Sheared aplite dyke at Station 33 (in horizontal plane). A narrow east-west striking shear zone that runs from top to bottom in the photograph separates the aplite dykes with a sinistral sense.

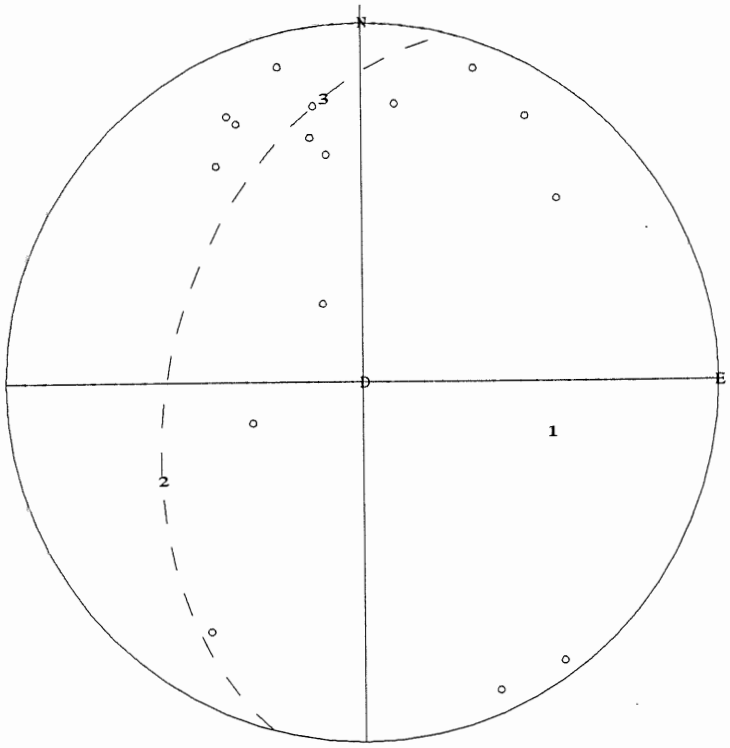

Figure 3.14 Poles to all shear zones in the Dunamagon Granite (16 points) showing that the shear zones are predominantly moderately to steeply dipping with some variation in strike (approximately east-west striking).

Figure 3.15 Strongly foliated rocks of the Ming's Bight Group in the Big Brook Shear Zone (Station 6, looking west). Numerous quartz pods are contained within the plane of the foliation.

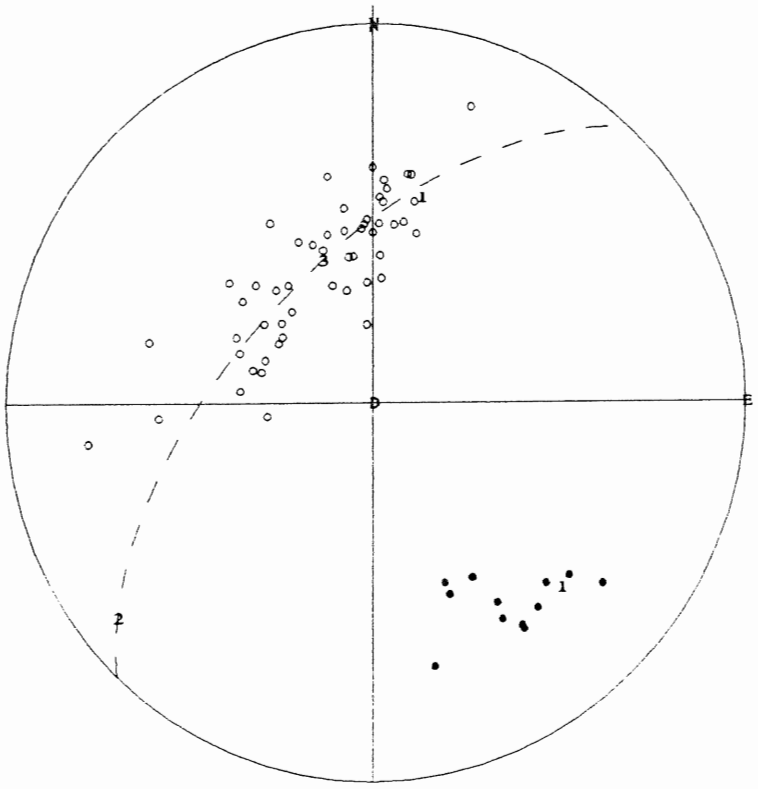

Figure 3.16 Poles to foliations (o), and lineations (●), in the Big Brook Shear Zone (53 points). The line is the best-fit great circle for the foliation. The foliation is northwest-southeast striking and moderately dipping. The lineation trends southwest and plunges moderately.

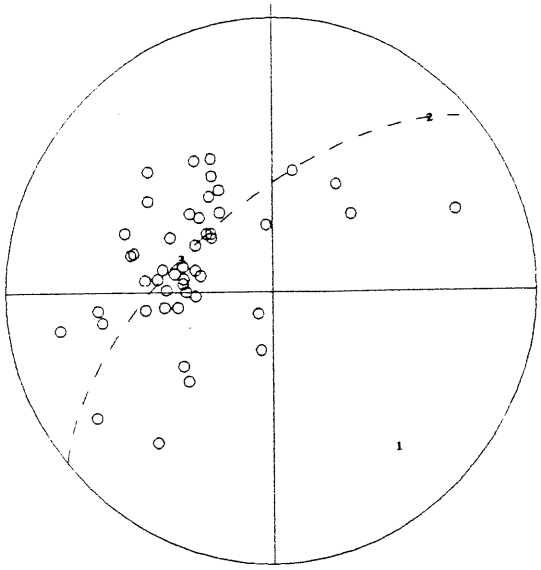

Figure 3.17 Poles to fold axial planes (48 points) in the Ming's Bight Group within the study area (near the Big Brook Shear Zone and on Pelée Point). The line represents the best-fit great circle.

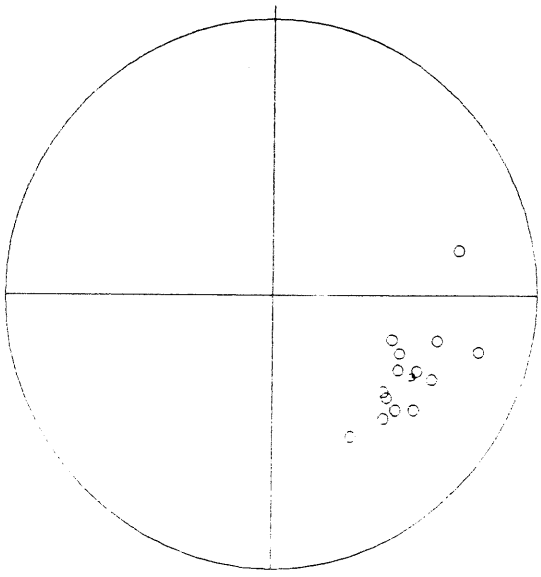

Figure 3.18 Southeast trending hinge lines (14 points) in the Ming's Bight Group within the study area (near the Big Brook Shear Zone and on Pelée Point).

aplite dykes. A section of mylonitized Peleé Point Schist occurs at the eastern end of the BBSZ .

3.9 Macroscopic Kinematic Indicators

The foliation is not asymmetric on the large-scale but, in some places, rotated feldspar crystals act as shear sense indicators, suggesting northward-verging movement. Asymmetric quartz boudins in the BBSZ (viewed in cross-section looking down the lineation) indicate dextral shearing. The Peleé Point Schist mylonite contains a dextral kinematic indicator (Fig. 3.19).

3.10 Structural Relationships

Figure 3.20 is a synoptic stereogram showing the orientation of the structures of the Dunamagon Granite (foliation, lineation), aplite dykes, quartz veins, mafic body orientation and foliation, Big Brook Shear Zone (foliation, lineation), and Ming's Bight Group (fold axial plane, hinge lines). All the planar features (foliations, dykes, mafic bodies, fold axial planes), with the exception of quartz veins, plot in the upper left quadrant of the stereogram, demonstrating the parallelism of these structures. The linear features (lineations, hinge lines) cluster in the lower left quadrant, indicating the similarity in orientations of these southeast trending features. The parallelism of the structures within the granite and the shear zone that defines part of its northern boundary suggests that the structures are genetically related and probably formed during the same episode of deformation.

3.11 Summary

Aplite dykes are the earliest of the cross-cuttting features in the Dunamagon Granite. The uncertainty of the origin of the mafic bodies creates problems in working out their relative ages. If the bodies are xenoliths, they must predate the aplite dykes. If the

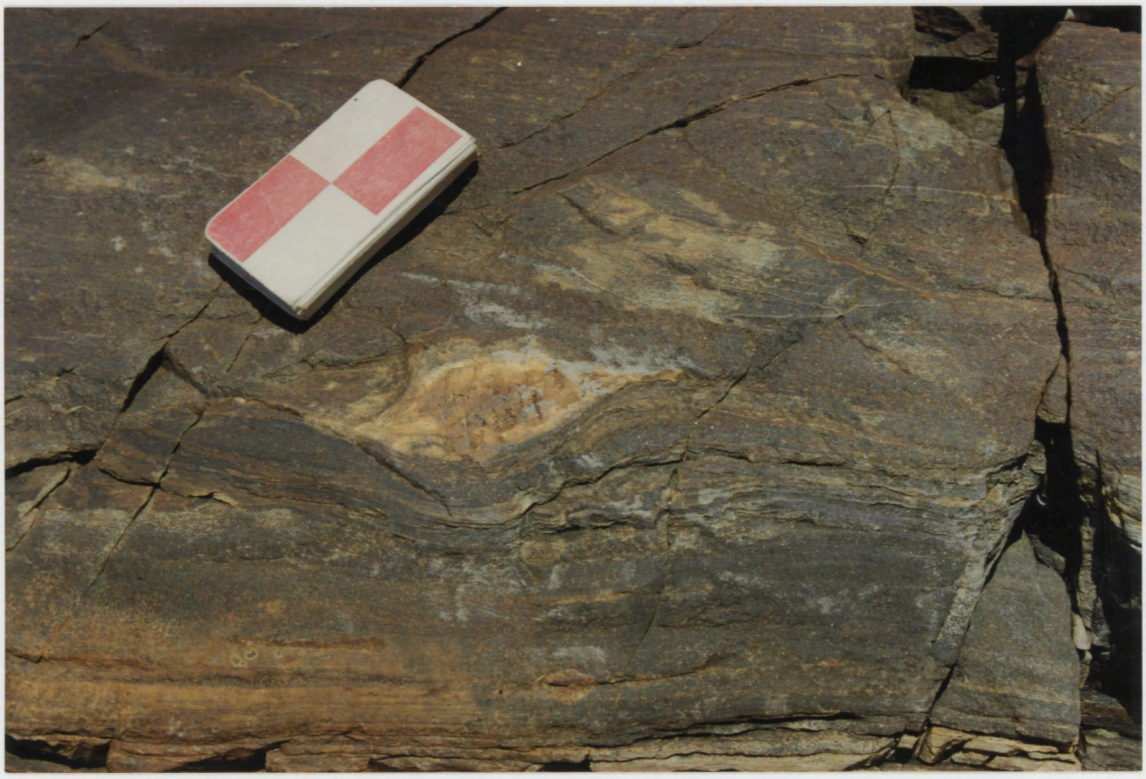

Figure 3.19 Dextral kinematic indicator in the Pacquet Harbour Group mylonite (foliation 080/54, lineation 125→56)at the eastern end of the Big Brook Shear Zone (Station 22, facing south). The dextral rotation indicates tops-to-north sense of overthrusting.

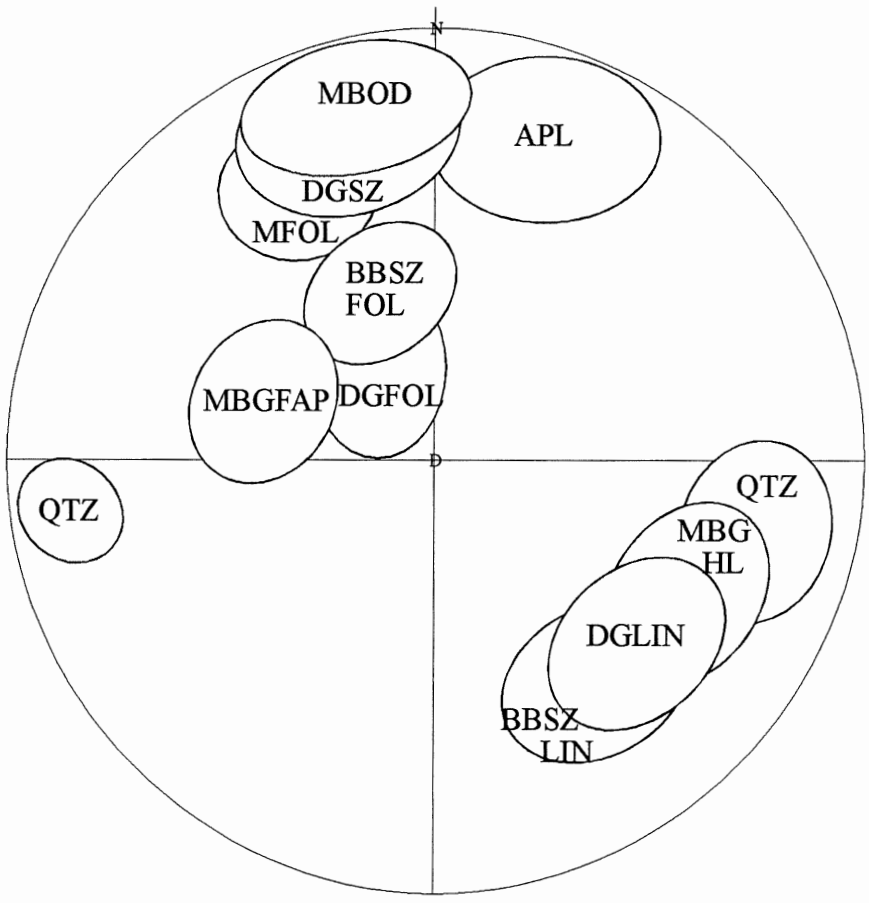

Figure 3.20 Orientation fields for major structures in the study area. See text for discussion. DGFOL=Dunamagon Granite foliation, DGLIN=Dunamagon Granite lineation, DGSZ=Dunamagon Granite shear zones, QTZ=quartz veins, APL=aplite dykes, MBOD=mafic body orientations, MFOL=mafic body foliations, BBSZFOL=Big Brook Shear Zone foliation, BBSZLIN=Big Brook Shear Zone lineation, MBGFAP=Ming's Bight Group fold axial planes, MBGHL=Ming's Bight Group hinge lines

mafic bodies are dykes, they probably post-date the aplite dykes and at least one generation of quartz veins. The foliation, lineation, and shear zones post-date the mafic bodies. The large and small shear zones are probably related to phases of ductile and brittle deformation events, respectively, with the brittle event post-dating the ductile event. Many generations of quartz veins are present; they cannot be constrained to one time period, and probably formed throughout the deformation history of the pluton. Parallelism of structures of the Dunamagon Granite and the Ming's Bight Group immediately to the north suggest the structures formed during the same deformation event, most likely the thrusting of the Dunamagon Granite and Pacquet Harbour Group. These field-based observations provide the basis for the structural study of a Dunamagon Granite. The next chapter provides information on microstructures and possible deformation mechanisms.

CHAPTER 4 MICROSTRUCTURES AND DEFORMATION MECHANISMS

4.1 Introduction

Chapter 3 presented the nature and orientations of macro- and mesostructures of the Dunamagon Granite. Microstructures and textures, on the scale of thin sections, provide information that cannot be gained by studying larger-scale structures. Microstructures reflect the mechanism(s) by which they form and, therefore, can be used to qualitatively deduce the temperature and stress conditions at the time of deformation. The microstructural criteria are the basis for deformation mechanisms proposed for the Dunamagon Granite.

4.2 Microstructures

The microstructures that develop during deformation are governed by deformation mechanisms, and these mechanisms are a function of strain rate and temperature of deformation. In granitoid rocks, quartz is usually the least competent phase and it deforms easily in response to stress, producing particular microstructures. These microstructures include deformation bands, deformation lamellae, twin boundaries, undulatory extinction, subgrain boundaries, grain shape preferred orientation (GSPO), and crystallographic (or lattice) preferred orientation (CPO or LPO) (Best 1982, Hobbs et al 1976).

4.3 Deformation Mechanisms

Various deformation mechanisms, dependent on temperature, strain rate, and stress, operate on a microscopic scale to produce permanent strain in rocks (Park 1989). . The eight main deformation mechanisms are dislocation glide, dislocation creep, rotational recrystallization, grain boundary migration (GBM) recrystallization, static recovery (annealing), cataclastic flow, pressure solution, and diffusional creep (Hobbs et al 1976,

Best 1982). Table 4.1 summarizes the combinations of microstructures for identifying deformation mechanisms. The microstructures in a rock are a result of an interaction of the processes described above.

Microstructures and deformation mechanisms can be broadly classified into two categories based on temperature or strain rate. At low temperature or high strain rate recovery and recrystallization are difficult (slow diffusion) and the crystals will exhibit evidence for strong internal deformation (flattened grains, deformation bands, deformation lamellae, and extremely high densities of dislocations (Hobbs et al 1976). At high temperature or lower strain rate, recovery is easier because diffusion is important. Intracrystalline distortion is less severe and recrystallization becomes more important. Grain growth may be apparent because of grain boundary recrystallization and enhanced mobility. Grains are elongate but not severely internally distorted (Best 1982).

4.4 Microstructures and Deformation Mechanisms in the Dunamagon Granite

4.4.1 Quartz Microstructures

The range of microstructures in the Dunamagon Granite reflects the inhomogeneity of deformation at observed macro- and mesoscopic scales. Table 4.2 summarizes the microstructures in each sample and the photomicrographs (Figs. 4.2-7) illustrate these structures. Figure 4.1 shows sample locations.

The microstructures in the Dunamagon Granite record two phases of deformation. The first, higher temperature event, is represented by elongate quartz ribbons composed of relatively few, large grains, little undulatory extinction, and "normal" (i.e. not sutured) grain boundaries, in a matrix of equant feldspar grains (Fig. 4.3). Microcline, typical of amphibolite grade recrystallization of K-feldspar, is present in the matrix. A second generation of quartz ribbons is formed by recrystallization of coarse quartz ribbons with a significant decrease in grain size.

	dislocation glide	dislocation creep	GBM recrystallization	rotation recrystallization	static recovery	cataclastic flow	pressure solution
deformation lamellae	few/ weak						
deformation bands	few/ weak	many/ strong					
mechanical twins	yes						
undulatory extinction	patchy or smooth	many/ strong			no, flat field extinction	patchy	
flattening of grains	weak	many/ strong					yes
GSPO	few/ weak	yes			no		
LPO		many/ strong	many/ strong	yes	few/ weak		
sub- and recrystallized grains		many		subgrains around un-recrystallized cores			
strain-free new grains			same size as grain boundary bulges				no
fine material crosses the crystal			in early stage			yes	
"beards" at low pressure ends of rigid grains							yes
insoluble residues							yes
sutured grain boundaries			yes				yes
polygonal/ blocky grains					yes		

Table 4.1 Checklist for identification of deformation mechanisms based on Simpson (1987). This table lists combinations of microstructures that are characteristic of each deformation mechanism. In most cases, at least one type of microstructure, or a particular combination of microstructures, is unique to a particular mechanism.

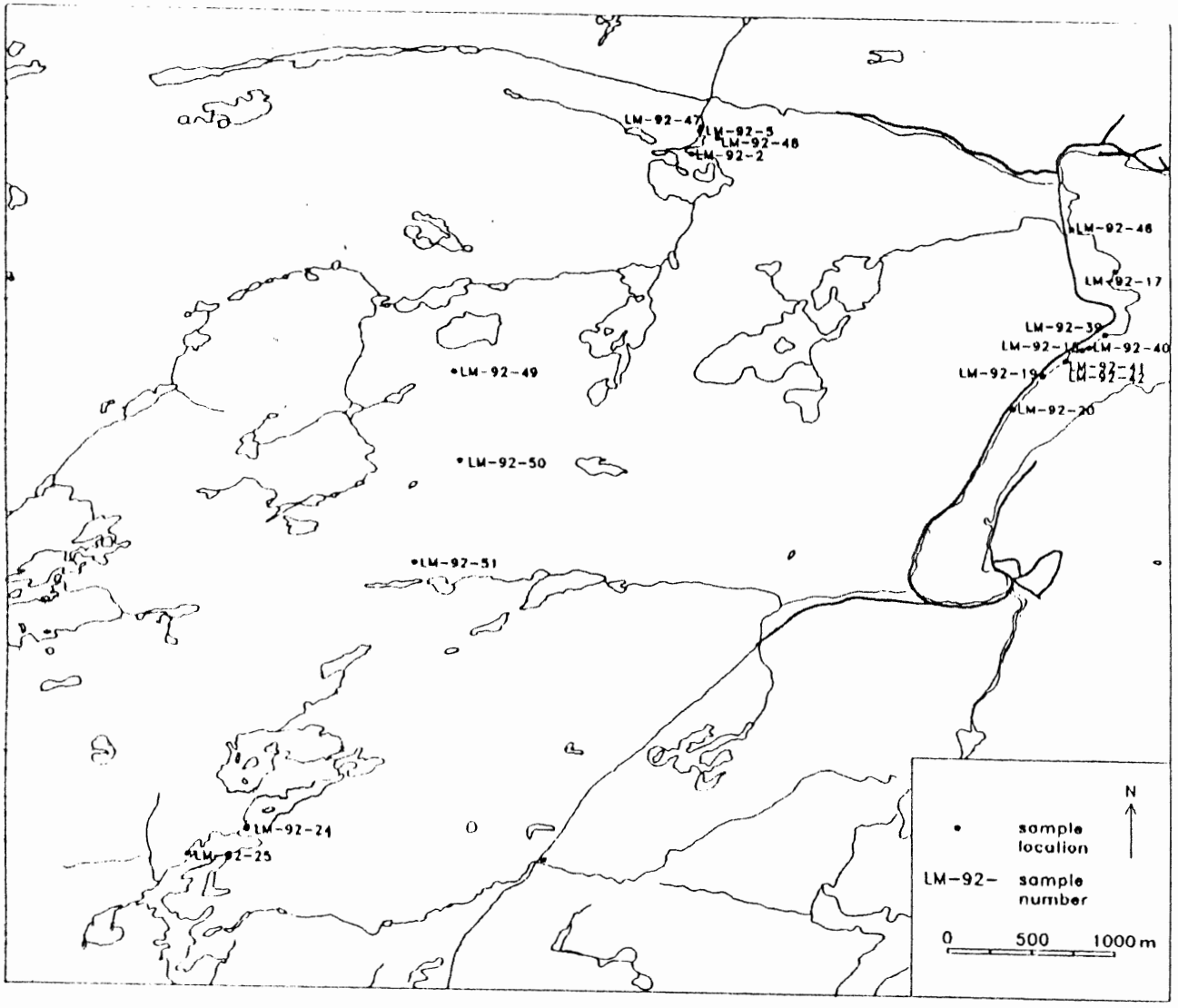

Figure 4.1 Thin section sample locations.

Figure 4.2 LM-92-51: least deformed sample of Dunamagon Granite, coarse-grained quartz and feldspar (Field of view = 10 x 14 mm).

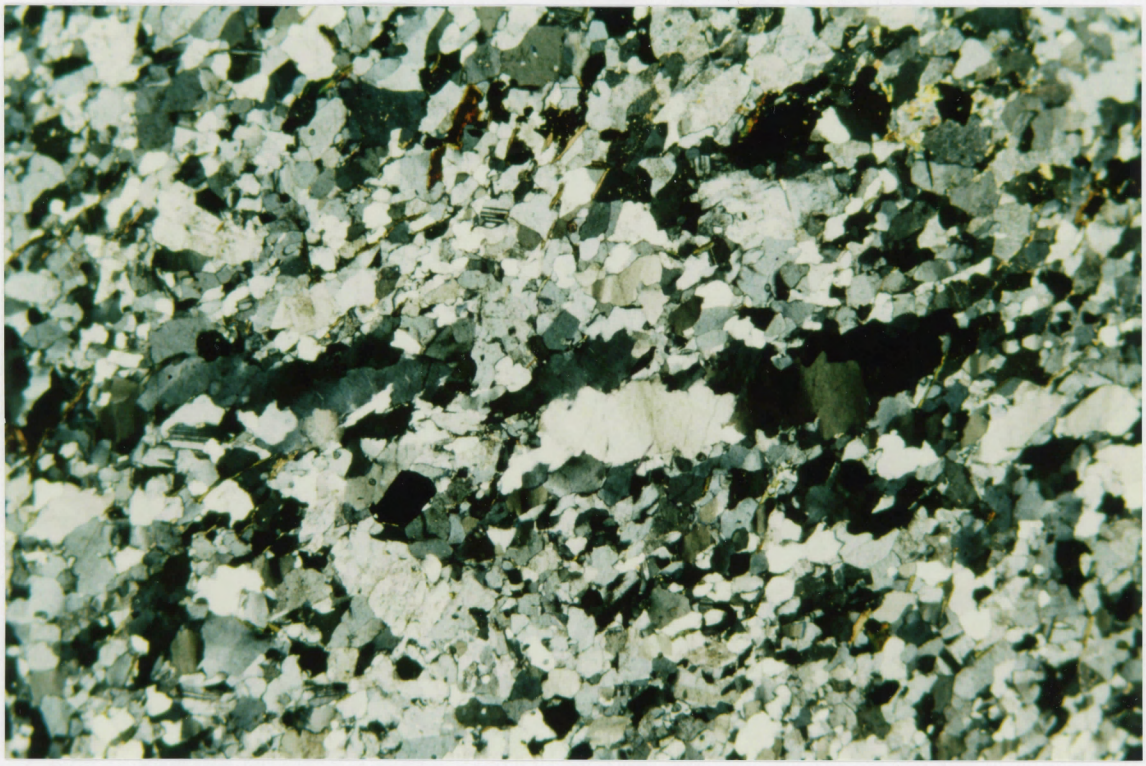

Figure 4.3 LM-92-20: showing a coarse quartz ribbon with a LPO (Field of view = 10 x 14 mm).

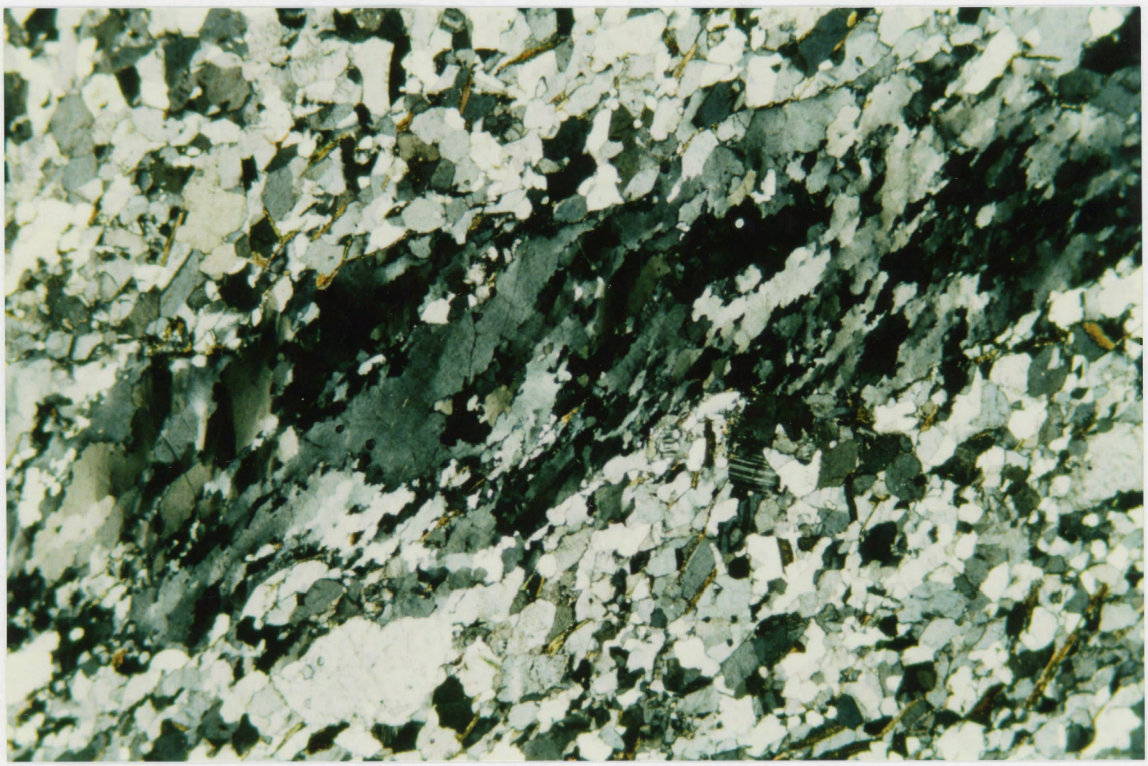

Figure 4.4 LM-92-20: quartz ribbon with strong LPO, GSPO, sutured grain boundaries (Field of view = 10 x 14 mm).

Figure 4.5 LM-92-40: quartz ribbon with strong LPO and GSPO, twinned K-feldspar porphyroclast (Field of view = 10 x 14 mm).

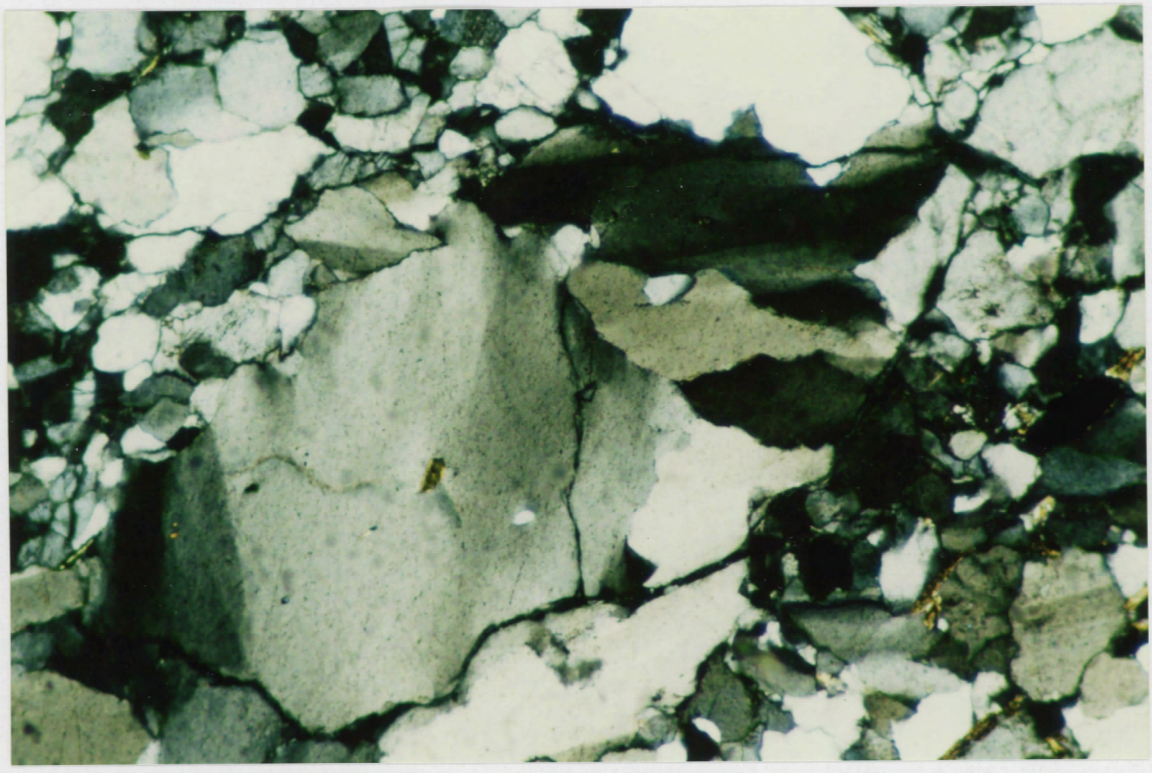

Figure 4.6 LM-92-2: undulatory extinction in quartz (Field of view = 3 x 4.5 mm).

Figure 4.7 LM-92-49: fractured K-feldspar porphyroclast with twinning and exsolution, quartz filling the fracture (Field of view = 10 x 14 mm)

These grains have a GSPO, sutured grain boundaries, strong undulatory extinction (which indicates that recovery is not as advanced), and a lattice-preferred orientation (Fig. 4.4). The long axis of the grains is inclined to the trace of the older quartz ribbons. Lattice-preferred orientation is evident in a flat stage. Table 4.2 summarizes these microstructures.

4.4.2 Deformation Mechanisms for the Dunamagon Granite

The types of microstructures present in the Dunamagon Granite suggest the occurrence of dislocation creep and grain boundary migration. Quartz in the samples exhibit many deformation bands, strong undulatory extinction, strong flattening of grains, grain shape preferred orientation, and strong lattice-preferred orientation, all typical of dislocation creep. Sutured grain boundaries and lattice-preferred orientation indicate grain boundary migration recrystallization. The microstructures associated with GBM (sutured grain boundaries, LPO) occur exclusively in the second generation of quartz ribbons representative of lower temperature deformation. The other microstructures (deformation bands, undulatory extinction, flattening of grains, GSPO, and LPO) represent a higher temperature phase of deformation in which the mechanism was dislocation creep.

4.5 Summary

Microstructures in the Dunamagon Granite include quartz ribbons, subgrains, grain shaped preferred orientation, crystallographic (lattice) preferred orientation, and undulatory extinction. There is evidence in the granite for two deformations. Dislocation creep produced the majority of microstructures during a higher temperature phase of deformation of the Dunamagon Granite, but grain boundary migration produced sutured grain boundaries and contributed to the lattice-preferred orientation in quartz ribbons. The lower temperature structures generated by grain boundary migration overprint the

sample LM-92-	2	5	47	17	18	19	20	39	40	42	49	51	25
deformation bands					✔		✔	✔		✔	✔		✔
undulatory extinction	✔	✔	✔	✔	✔		✔	✔	✔	✔	✔	✔	✔
flattening of grains				✔	✔	✔	✔	✔		✔	✔		✔
GSPO							✔			✔	✔		✔
LPO		✔		✔	✔	✔	✔	✔		✔	✔		✔
sub- and recrystalliz-ed grains				✔	✔		✔		✔	✔	✔		✔
sutured grain boundaries		✔		✔	✔						✔		
geograph-ical area	NC	NC	NC	EC	EC	EC	EC	EC	EC	EC	CR	CR	SC
Figure number	4.6						4.3, 4.4		4.5			4.2	

Table 4.2 Microstructures in the Dunamagon Granite from across the pluton (NC = northern contact, EC = eastern coast, CR = central region, SR = southern region)

earlier structures and are only found in samples from the northern portion of the pluton (along the coast, in the central region, and near the northern contact).

CHAPTER 5 METAMORPHISM

5.1 Introduction

The Dunamagon Granite experienced two deformation events. Distinct metamorphic assemblages are lacking in the granite, but the mafic bodies have also recrystallized to form new mineral assemblages representing peak metamorphic conditions. This chapter discusses the correlation of the temperature of metamorphism with minerals present in the mafic rocks (mafic bodies, Pacquet Harbour Group) near the Dunamagon Granite. Microprobe analyses of minerals of equilibrium assemblages (Appendix E) potentially permit quantitative estimation of P-T conditions, but time limitations have prevented further work on this topic.

5.2 Dunamagon Granite

The minerals present in the Dunamagon Granite are quartz, K-feldspar, plagioclase, biotite, chlorite, titanite, magnetite, epidote, sericite (in feldspars), white mica (in matrix), zircon, with minor tourmaline and amphibole (hornblende). Metamorphic minerals in the Dunamagon Granite include biotite, recrystallized feldspar, and later sericite and chlorite. In most cases, biotite defines the foliation. The colour of biotite ranges from olive-green to red-brown, reflecting changes in the titanium content of the biotite as a function of metamorphic grade. The chlorite and sericite are low-grade alteration minerals.

5.3 Mafic Bodies

The mafic bodies have completely recrystallized at epidote-amphibolite grade and the mineral assemblage epidote-hornblende-biotite-quartz-plagioclase represents the peak metamorphism. Decussate biotite defines a crenulated S_1 foliation (Fig. 5.1). Relatively fine-grained epidote and titanite follow S_1, and occur as inclusion trails in the hornblende.

Figure 5.1 LM-92-41: mafic body with a crenulation defined by biotite; note the presence of epidote (Field of view = 10 x 14 mm)

Some biotite grew axial planar to the crenulation (S_2). Although the crenulation is pervasive, it varies somewhat in orientation.

5.4 Pacquet Harbour Group North of the Dunamagon Granite

The mylonite of Pacquet Harbour Group at the eastern end of the Big Brook Shear Zone is completely recrystallized. Green hornblende comprises most of the rock, and defines a foliation that alternates with leucocratic layers. A folded leucocratic vein containing prehnite, calcite, quartz, and epidote follows the foliation. Prehnite is a metamorphic mineral characteristic of low temperature metamorphism associated with hydrothermal alteration or burial metamorphism (Yardley 1989). This rock was deformed at low temperature after the formation of prehnite. The presence of recrystallized amphibole and prehnite in the same sample (Fig. 5.2) strongly suggests two metamorphic events: the first event at amphibolite facies conditions, and the second at low temperatures and pressures (Fig. 5.3). This is consistent with the results of the microstructural study.

5.5 Pacquet Harbour Group at the Southern Boundary of the Dunamagon Granite

The minerals in this sample include fine-grained green hornblende which defines a foliation, completely altered feldspar porphyroclasts, and metamorphic magnetite. A prehnite vein cuts across the foliation, and provides evidence of a low temperature event that postdates the foliation in the amphibolite. Evidence for an early, high temperature event and a later, low temperature, possibly hydrothermal event, is confirmed.

5.6 Metamorphism and Deformation

In the Dunamagon Granite two deformation phases are recognized by microstructural assemblages. The first deformation event occurred at high (amphibolite grade) temperatures, characterized by coarse quartz ribbons with a lattice-preferred

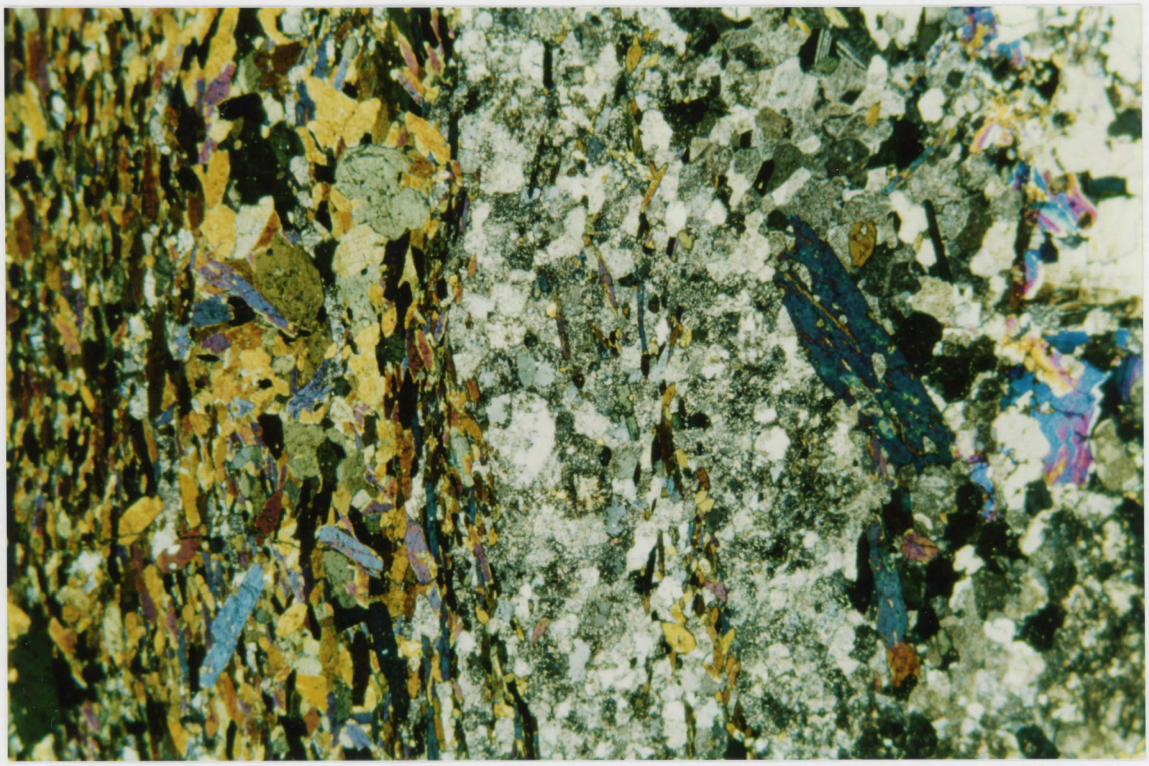

Figure 5.2 LM-92-46: recrystallized amphibole defining a strong foliation (left) and a leucocratic vein containing prehnite (bright blue-purple mineral at very right of photomicrograph) (Field of view = 10 x 14 mm)

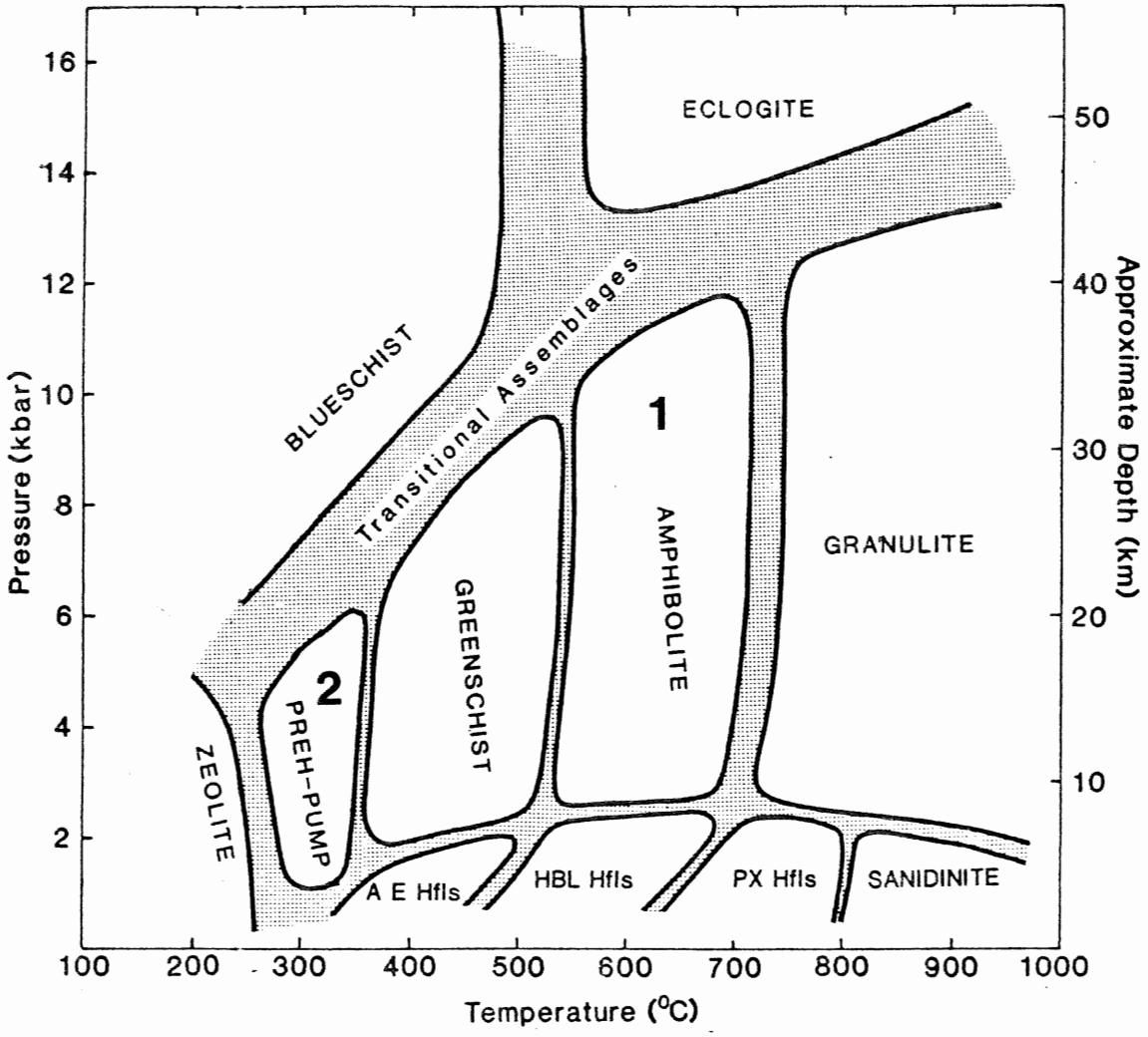

Figure 5.3 Pressure-temperature diagram showing the fields of the various metamorphic facies. Abbreviations used are: Hfls = hornfels, AE = albite-epidote, HBL = hornblende, PX = pyroxene, PREH-PUMP = prehnite-pumpellyite (Yardley 1989). The numbers represent early, high temperature (1) and later lower temperature (2) events.

orientation. Microstructures in mafic rocks differ from those in the granite because mafic rocks respond differently to stress than quartz-rich rocks. Quartz in the granite qualitatively records the temperature of deformation, but the mafic bodies respond by recrystallizing under sufficiently high temperatures. High temperature microstructures in the Dunamagon Granite and high temperature metamorphic assemblages are related to the same event. A similar correlation exists between low temperature structures in the granite and the low temperature metamorphism associated with a second deformation event, and overprinting of the structures and minerals of the first event.

5.7 Summary

The Dunamagon Granite does not contain a metamorphic assemblage that can be used to quantitatively constrain metamorphic conditions, however the mafic rocks that are in contact with the Dunamagon Granite do preserve diagnostic assemblages. Recrystallization of amphibole in the mafic bodies and the Pacquet Harbour Group at high temperatures corresponds to the high temperature quartz microstructures in the Dunamagon Granite. Prehnite in the Pacquet Harbour Group samples indicates low temperature metamorphism which may correlate with low temperature deformation and alteration in the Dunamagon Granite.

CHAPTER 6 DISCUSSION

6.1 Introduction

The Dunamagon Granite shares part, if not all, of its deformation history with the Pacquet Harbour Group and Ming's Bight Group, and the relationship of the Dunamagon Granite to these groups is important for constraining the relative timing of events along the easterly portion of the Baie Verte Line. This chapter addresses possible interpretations for the nature of the contact of the Dunamagon Granite with the Ming's Bight Group, and the sense of movement of the groups. A discussion of possible origins of the mafic bodies follows.

6.2 Re-interpretation of the Relationship between the Dunamagon Granite and the Ming's Bight Group

6.2.1 Contact Relations and Significance

The relationship of the Dunamagon Granite to the Ming's Bight Group has implications for the juxtaposition of the Humber and Dunnage Zones and the timing of tectonic events in this area. The Dunamagon Granite intrudes the Pacquet Harbour Group, but the nature of the contact between the Dunamagon Granite and the Ming's Bight Group is controversial. Three possibilities exist for the origin of this contact:

1. The Dunamagon Granite intruded the Ming's Bight Group as a "stitching pluton" joining the Ming's Bight Group and the Pacquet Harbour Group, and thus the age of intrusion post-dates the juxtaposition of the groups. In this case the pegmatites in the Ming's Bight Group would be related to the intrusion of the Dunamagon Granite.
2. The Dunamagon Granite intruded the Ming's Bight Group and the intrusive contact has since been tectonically activated as a plane of weakness.

Pegmatites in the Ming's Bight Group may be related to the intrusion or to partial melting of the granite during shearing. The Dunamagon Granite initially intruded the Ming's Bight Group and the Pacquet Harbour Group, therefore the age of intrusion constrains the joining of the groups. A Devonian titanite age (Dunning and Cawood, submitted) may represent the time of reactivation of the Baie Verte Line.

3. The Dunamagon Granite is in tectonic contact only with the Ming's Bight Group. The age of intrusion is, therefore, a maximum age of the juxtaposition of the Humber and Dunnage Zones, and the titanite age may be related to a higher temperature deformation event. Pegmatites may be related to shearing of the granite or may be from previous deformation of the Ming's Bight Group and completely unrelated to the Dunamagon Granite.

Accurate determination of the nature of the contact requires careful consideration of the available evidence. Evidence in favour of intrusion includes pegmatites in the Ming's Bight Group and xenoliths of Ming's Bight Group (DeGrace et al 1976) in the Dunamagon Granite, the latter not confirmed by this study. Evidence for a tectonic contact includes the presence of the Big Brook Shear Zone along the contact of the granite with the Ming's Bight Group, the presence of mylonite at the eastern end of the shear zone, a strong correlation of structures within the granite and the structures that constrain the northern boundary. Evidence for contact metamorphism is absent in the Ming's Bight Group but may have been obliterated by shearing. Based on weak evidence for an intrusive contact (xenoliths in the Dunamagon Granite, pegmatites in the Ming's Bight Group), and strong evidence for a tectonic contact (Big Brook Shear Zone, structures in the granite parallel structures at its contacts), it is not possible to distinguish between the second and third possibilities.

6.2.2 Thrusting

The combination of structures in the Dunamagon Granite, the Pacquet Harbour Group mylonite north of the granite, and the Big Brook shear zone can be used to infer a sense of movement along the tectonic contact of the Dunamagon Granite with the Ming's Bight Group. Asymmetric K-feldspar porphyroclasts in the granite, viewed perpendicular to the foliation and parallel to the lineation, in vertical erosion surfaces indicate motion of top side to the north. The sense of shear observed in horizontal section in the mylonite is dextral. In the Big Brook shear zone dextral sense of shear is inferred from quartz boudins, and the main foliation strikes easterly, dipping moderately to steeply to the south. The lineation in the Dunamagon Granite (which plunges obliquely down dip of the foliation in a southeast direction), combined with the orientation of the foliation in the granite, mylonite, and Big Brook shear zone, and a dextral sense of shear in each case, indicates that motion along the contact had a thrust sense (Fig. 6.1). This suggests that the Dunamagon Granite and the Pacquet Harbour Group were thrust onto the Ming's Bight Group.

6.3 Mafic Bodies

The structures and metamorphic assemblages in these bodies are related to deformation they have undergone while in the Dunamagon Granite, and provide important information about the conditions of deformation. The origin of the mafic bodies is uncertain. Whether they are dykes or xenoliths affects any interpretation about their relative age and deformation. If the bodies are xenoliths, the S_1 fabric may be a foliation of the protolith preserved in the xenolith and, therefore, not related to the deformation of the Dunamagon Granite. The Pacquet Harbour Group is a reasonable source for mafic xenoliths, and it had a foliation at the time of the intrusion of the Dunamagon Granite.

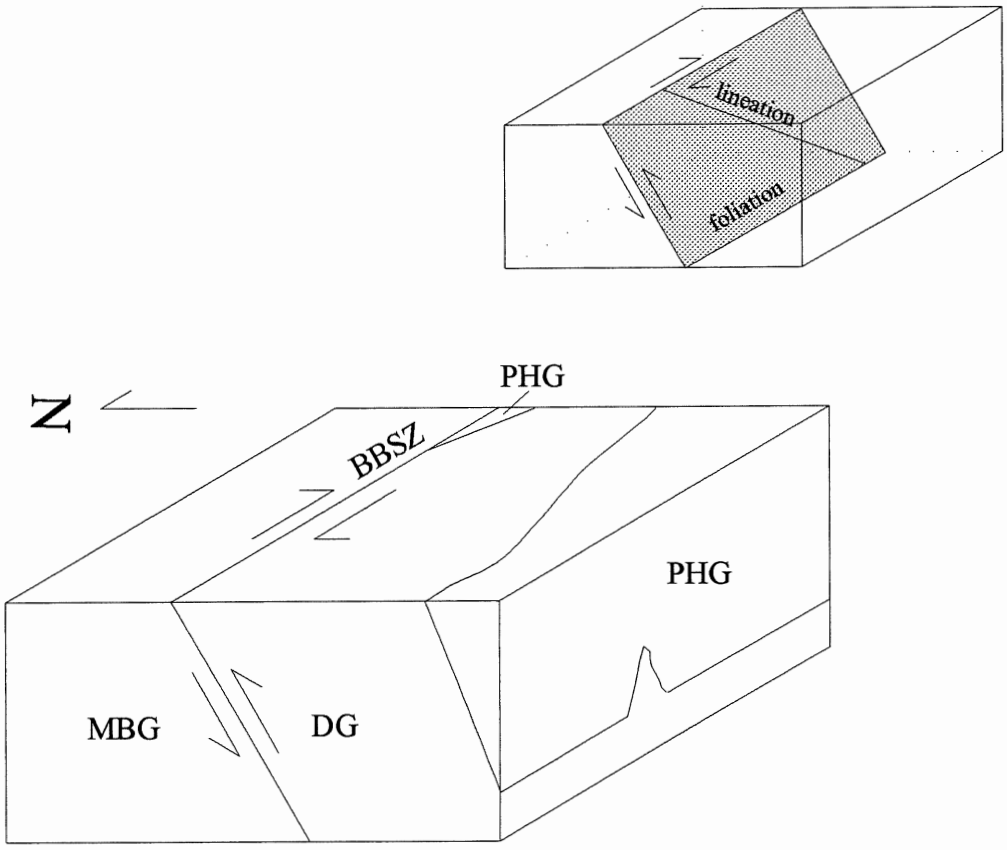

Figure 6.1 Schematic block diagram of overthrusting of the Dunamagon Granite and Pacquet Harbour Group. Dextral shearing along the Big Brook Shear Zone and tops-to-north sense of motion along foliations combine as oblique thrusting.

If the mafic bodies are dykes, their fabrics (S_1, S_2) indicate that they have been affected by two deformation events: the first at a temperature high enough to cause recrystallization accompanied by the formation of S_1, and the second, lower temperature phase that produced the S_2 crenulation. Two phases of deformation in the dykes are consistent with microstructural evidence in the Dunamagon Granite (cf. LM-92-20, Chapt. 4), but S_1 and S_2 are parallel in the granite and perpendicular in the mafic bodies. Further work is needed to clarify the issue.

6.4 Summary

The contact of the Dunamagon Granite with the Ming's Bight Group is important to understanding the relationship of the groups on either side of this portion of the Baie Verte Line in the study area. The contact is tectonic, marking a shear zone along which the Dunamagon Granite and the Pacquet Harbour Group have been thrust to the north. The age of the intrusion of the Dunamagon Granite may be a maximum, not a minimum, age of the juxtaposition of the Humber and Dunnage Zones.

CHAPTER 7 CONCLUSIONS

The Dunamagon Granite is a Silurian pluton in which tectonic structures developed (foliations, lineation, shear zones). The orientation of these structures and those of the aplite dykes, quartz veins, and mafic bodies is easterly-striking. The lineation in the granite and the intersection lineation of aplite dykes give the orientation of the stretching direction which was southeast-northwest. Microstructures record phases of high and low temperature deformation . Within mafic bodies in the granite, the equilibrium assemblage epidote-hornblende-biotite-quartz-plagioclase reflects the peak metamorphic conditions of the higher temperature deformation event. Prehnite in veins in the Pacquet Harbour Group indicates later, low temperature alteration.

The Dunamagon Granite intruded the Pacquet Harbour Group. The contact of the Dunamagon Granite with the Ming's Bight Group is tectonic along the Big Brook shear zone This contact may have been an intrusive contact that served as a plane of weakness to accommodate deformation. The Dunamagon Granite and Pacquet Harbour Group appear to be thrust over the Ming's Bight Group along this contact. If the Dunamagon Granite was brought into contact with the Ming's Bight Group by thrusting, then the age of intrusion (429 Ma) is a maximum, not a minimum, age for the juxtaposition of the Ming's Bight Group and Pacquet Harbour Group, and therefore, for the juxtaposition of the Humber and Dunnage Zones in this area.

Further Work

A thorough investigation of the western boundary of the Dunamagon Granite, where the contact with the Ming's Bight Group is not defined by the Big Brook shear zone, may clarify whether or not the Dunamagon Granite intruded the Ming's Bight Group prior to thrusting.

Quartz c-axis measurements are potentially very useful for determining the orientation and temperature conditions of deformation, and the exact deformation mechanism responsible for deformation in the Dunamagon Granite. Also, kinematics can be studied using the second generation grain shape preferred orientation of quartz.

Detailed study of the pegmatites in the Ming's Bight Group and of granite dykes in the Pacquet Harbour Group may help to determine whether or not these features are related to the intrusion of the Dunamagon Granite.

Pressure and temperature conditions of peak metamorphism can be calculated based on the electron microprobe analysis of mineral assemblages in the mafic bodies. Microprobe data was acquired during this study but time limitations prevented thermobarometric calculations. The data are included in Appendix E.

Analysis of the shape-fabric of the granite and the relative age of shear zones with respect to wall-rock fabrics should provide information about the deformation path of the Dunamagon Granite, and whether it underwent transpression or simple shear.

REFERENCES

Baird DM (1951) The geology of the Burlington Peninsula, Newfoundland, Geological Survey of Canada, Paper 51-21, 70 p

Best MG (1982) Igneous and Metamorphic Petrology. W.H. Freeman and Co., NewYork, 630p

Church WR (1969) Metamorphic rocks of the Burlington Peninsula and the adjoining areas of Newfoundland and their bearing on continental drift in the North Atlantic. In: North Atlantic Geology and Continental Drift. Kay M (ed) American Association of Petroleum Geologists, Memoir 12, pp 212-233

Dallmeyer RD, Hibbard J (1984) Geochronology of the Baie Verte Peninsula, Newfoundland: Implications for the tectonic evolution of the Humber and Dunnage Zones of the Appalachian Orogen. J of Geol 92: 489-512

De Grace JR, Kean BF, Hsu E, Green T (1976) Geology of the Nippers Harbour map area (2E/13), Newfoundland. Newfoundland Department of Mines and Energy, Mineral Development Division, Report 76-3, 73 p

Dunning GR and Cawood PA (1993) Silurian granitic plutonism on the Baie Verte Peninsula, Newfoundland. Submitted to Journal of the Geological Society of London

Hibbard J(1982) Significance of the Baie Verte Flexure, Newfoundland. Geol Soc Am Bull 93: 790-797

Hibbard J (1983) Geology of the Baie Verte Peninsula, Newfoundland, Memoir 2. Mineral Development Division Department of Mines and Energy, Government of Newfoundland and Labrador, 279p

Hobbs BE, Means WD, Williams PF (1976) An Outline of Structural Geology. John Wiley and Sons, New York, 571p

Kennedy MJ (1975) Repetitive orogeny in the northeastern Appalachians- New plate models based upon Appalachian examples. Tectonophysics 28: 39-87

Neale ERW (1958) Nippers Harbour, Newfoundland. Geological Survey of Canada, Map 22- 1958

Park RG (1989) Foundations of Structural Geology, 2nd ed. Blackie and Son Ltd., Glasgow, 148p

Simpson C (1986) Determination of movement sense in mylonites. J Geol Ed 34: 246-261

Williams H (1978) Tectonic lithofacies map of the Appalachian orogen. Memorial University of Newfoundland, Map 1

Yardley BWD (1989) An Introduction to Metamorphic Petrology. Longman Scientific and Technical, Essex

APPENDIX A

Structural Measurements

Dunamagon Granite

station	foliation	lineation	quartz veins	aplite dykes	mafic bodies	mafic foliation	shear zone
10				097/66			
-			294/37				
11	160/9				055/73 095/60	065/80 067/66	
11A	055/25	157→27 151→36 141→18	188/58 240/85				
12	068/25				078/65	147/45	
12A	054/18		225/63		224/85	358/56	
12B	298/32			101/82			
12C			054/64	160/75 330/40			
12D	310/30						
13	075/18						
14	332/26		220/60	304/74 335/54			
-			220/52				
-			201/48				
15	025/21		094/73 192/48		078/69 075/65	078/46 082/74	
16	116/46						
17	310/25	143→21					
18	222/9		184/54				
-		087→36			247/64 275/55	302/45	
-			175/75				
19					063/84	063/70	
20	023/21						
-	323/20						
-			190/72				
-			182/83				
-	073/39						
21	066/44	134→44					081/54
23			116/75		272/82		

station	foliation	lineation	quartz veins	aplite dykes	mafic bodies	mafic foliation	shear zone
24	018/30						246/83 234/85
25	062/58		219/74				064/69
26	138/78	127→45	127/23				110/82
-	062/17			101/53			
27	137/64			125/63			137/64
28	030/24 114/80						063/72 075/80
29				060/75			056/62
30	005/9	095→14	337/60				080/67
31	100/80						302/70
32	080/51		346/56		296/80	098/41 356/43	078/59
33	094/77	110→45	341/77 193/74				
34	002/16		177/76				063/20
35	358/20						
36	032/22						
37	060/16						097/67
38	000/20		151/77 090/23				
48A	060/52						
49A	129/17						
50A	137/21						
51A	150/17						
59	140/31						
60	085/52						
61	074/48						
62	084/55						
63	070/55		150/70				
64	074/57						
65	072/38						
66	078/28						
67	091/47						
68	067/11						
69	083/23						
70	108/30						
71	054/14						
72	092/35						

station	foliation	lineation	quartz veins	aplite dykes	mafic bodies	mafic foliation	shear zone
73	069/27						
75	065/37						
76	166/17						
77	268/26 263/40						
78	238/53						
79	222/40						
80	167/40						
81	255/42						
82	059/26						
83	072/33						
84	045/27						
85	046/26						
86	067/14						
misc	028/27 076/41 085/32 280/17 082/68 062/56						

Pacquet Harbour Group

station	foliation	fold axial plane	crenula-tion	hinge line	mafic body	mafic foliation
22	080/54	025/10 012/25 030/35	350/32	100→27	087/45	092/38 320/56
39	048/35			147→18		
45A	045/58					
46A	051/68					
47A	058/38					

Ming's Bight Group

station	foliation	fold axial plane	hinge line	lineation	quartz vein	actinolite pod	mafic dyke foliation
-	102/45 352/67						
6A	092/45	122/38					
7A	095/45						
8A	088/40						
9A	094/47						
10A	076/25						
11A	094/27						
12	093/49						
6	087/26			166→30 127→23			
7	086/38 100/40 085/17				310/32		
-	090/37	137/34					
8	087/39 093/32			145→30			
9	097/39 105/38 095/43 080/38			147→38 145→29			
41	080/32						
-	042/28 056/50	084/20					
42	109/70	044/32	105→20				
43	100/51 099/51			140→31			
44	090/52 068/37 093/54	055/35		130→31	253/52		
45	092/39	157/65				130/40	
46	081/43						082/31
47	093/44 078/51	055/29 042/26					

station	foliation	fold axial plane	hinge line	lineation	quartz vein	actinolite pod	mafic body foliation
48	037/37	043/35 061/35 061/40 010/31 058/47 021/50 308/60	105→35 117→32 130→44 117→38 137→38 150→40	157→48 148→34 157→45 135→34 076→30			
49		345/56 015/45 015/25	120→44 132→27 128→32				
50	064/39						
51	074/38	040/27					
52	062/30	078/45					011/39
53	048/33	040/25					
54		027/36				078/35 352/32 084/20	
55	035/25						
56	031/25						
57	082/32						
58	070/27	100/37					
87	353/24	350/55 005/40 325/70	110→50 077→28 131→42				
88		352/40 314/38 030/28 351/30 282/18 305/8 005/28 064/45					
89	015/26	357/24					
90		350/70 043/54 015/45					
91	356/49						

station	foliation	fold axial plane	hinge line	lineation	quartz vein	actinolite pod	mafic dyke foliation
92	005/30	006/36 000/27	114→46				
93		015/29					
94	015/53	014/46					
95	020/36						
96	048/33 010/33	352/34					
97	047/27 015/28	008/28					
98	053/32 025/34	011/23					
99	021/26 020/32	012/23					
100	044/37						
101	039/42	035/48					
102	035/30						
103	040/27	321/36					
104	059/46	001/33					

APPENDIX B

Detailed thin section descriptions for all Dunamagon Granite samples

sample number	LM-92-2	LM-92-5	LM-92-17	LM-92-18	LM-92-19	LM-92-20
biotite	pale brown, ragged	dark red-brown	brown	brown	green	brown
chlorite	yes	rare	yes	yes	yes	yes
K-spar porphyro-clasts	yes, exsolution	yes	yes, exsolution twinning	yes, exsolution twinning	yes	yes
sericite	yes	yes, esp. in cores of fsp	yes	yes	yes	
titanite			yes		yes, idioblastic	yes
magnetite	yes		yes	yes	yes	yes
quartz ribbons				yes, coarse		yes, fine and coarse
undula-tory extinction		yes	yes	yes		yes
sutured grain boundar-ies		yes	yes	yes		
GSPO						yes
LPO		yes	yes	yes	yes	yes
subgrains			yes	yes		yes
flattening of grains			yes	yes	yes	yes
grain size	fine	fine	coarse	coarse	medium	medium
miscellan-eous	tourmaline	zoning in matrix fsp	myrmekite tourmaline biotite wraps around grains	magnetite is associated with titanite	myrmekite K-spar p'clasts are aggregat-es	sample from a shear zone, two types of quartz ribbons (see text)

sample number	LM-92-25	LM-92-39	LM-92-40	LM-92-42	LM-92-47	LM-92-49
biotite	olive-brown	greenish-brown	olive-brown	green	green-brown	tan
chlorite		yes	yes	yes		yes
K-spar porphyro-clasts	yes, exsolution twinning	yes, exsolution twinning	yes, exsolution twinning	yes, exsolution	yes, twinning	yes, exsolution twinning
sericite	yes	yes		yes	yes	yes
titanite		yes	yes	yes		yes
magnetite	yes	yes		yes	yes	yes
quartz ribbons	yes, fine	yes, coarse		yes, coarse		yes, fine
undula-tory extinction	yes	yes	yes	yes	yes	yes
sutured grain boundar-ies						yes
GSPO	yes			yes		yes
LPO	yes	yes		yes		yes
subgrains	yes		yes	yes		yes
flattening of grains	yes	yes		yes		yes
grain size	coarse	med to coarse	fine	medium	medium	medium
miscellan-eous	fsp p'clasts are fractured, biotite and quartz ribbons wrap around p'clasts		tourmaline biotite sheared in quartz ribbons	fabric wraps around p'clasts	fsp p'clasts much smaller than in other samples	hornblen-de epidote

sample number	LM-92-51
biotite	brown
chlorite	yes
K-spar porphyroclasts	yes, exsolution
sericite	yes
titanite	
magnetite	
quartz ribbons	
undula-tory extinction	yes
sutured grain boundaries	
GSPO	
LPO	
subgrains	
flattening of grains	
grain size	very coarse
miscellan-eous	least deformed sample, microcline

APPENDIX C

Bulk geochemical analyses of the Dunamagon Granite from DeGrace et al (1976)

sample	SiO2	TiO2	Al2O3	Fe2O3	FeO	MnO	MgO	CaO	Na2O	K2O	P2O5	L.I.
JRD 74-52	73.4	0.23	13.1	0.01	1.80	0.04	0.25	0.71	3.83	4.78	0.28	0.40
JRD 74-55	75.7	0.20	12.3	1.03	0.22	0.02	0.09	0.40	3.59	4.63	0.07	0.43

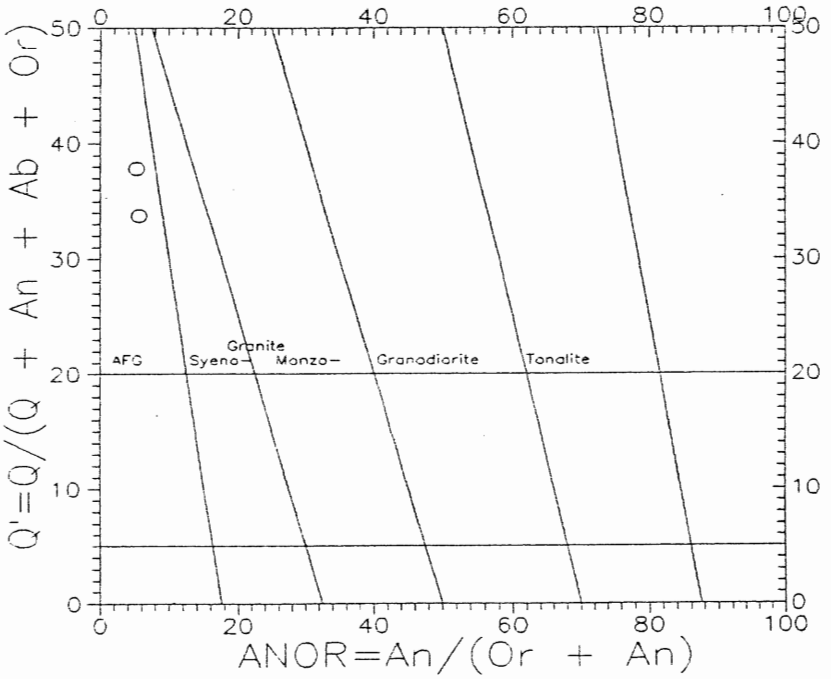

Classification of the Dunamagon Granite: Alkali feldspar granite

APPENDIX D

Published Abstracts:

Jamieson RA, Anderson S, and McDonald L (1993) Slip on the Scrape-An Extensional Allochthon east of the Baie Verte Line, Newfoundland. Geol. Soc. Am. Abstracts with Programs, 25:26

Jamieson RA, Anderson S, McDonald L, and Goodwin L (1993) Silurian Extension along the Humber-Dunnage Boundary Zone, Baie Verte Peninsula, Newfoundland. In: Late Orogenic Extension in Mountain Belts, Abstracts, Document du Bureau de Recherches Géologiques et Minières no. 219:102

№ 4221

SLIP ON THE SCRAPE - AN EXTENSIONAL ALLOCHTHON EAST OF THE BAIE VERTE LINE, NEWFOUNDLAND

JAMIESON, R.A., ANDERSON, S., & McDONALD, L., Department of Earth Sciences, Dalhousie University, Halifax, Nova Scotia, Canada, B3H 3J5

The Baie Verte Line (BVL) of northwestern Newfoundland is a complex fault zone that separates late Proterozoic - early Paleozoic continental margin rocks of the Humber Zone from accreted early Paleozoic volcanic arcs of the Dunnage Zone. Although this boundary is widely regarded as the Taconian (Ordovician) suture along which the Iapetus Ocean closed, recent structural, seismic, and geochronological evidence suggests that this interpretation requires substantial modification. Many puzzling features of the regional geology can be explained if an episode of Silurian regional extension followed initial overthrusting and preceded Acadian thrusting and strike-slip faulting. Field work east of the BVL in 1992 focussed on the Ming's Bight Group, a Fleur de Lys Supergroup equivalent on the "wrong" side of the BVL, and its contacts with adjacent units. We documented extension on faults bounding the Point Rousse ophiolite complex, including the Scrape "Thrust", and confirmed the presence of a normal fault on the western edge of the Silurian Burlington Granodiorite. We suggest that the Ming's Bight Group may have been pulled off the Fleur de Lys belt during post-collision extension and that the Point Rousse ophiolite may now represent an extensional klippe. The Silurian Dunamagon Granite is thrust over the Ming's Bight Group. This thrust, which may be of Acadian age, reworks an earlier, possibly extensional, mylonite zone separating the Ming's Bight and Pacquet Harbour Groups. The Flat Water Pond and Micmac Lake Groups, which occupy a narrow belt immediately east of the BVL, may represent graben-fill deposits formed during Silurian extension and deformed during Acadian thrusting. The preliminary interpretation presented here, which is compatible with a wide range of structural, seismic, geochronologic, and metamorphic data, awaits testing by further field and analytical work.

SILURIAN EXTENSION ALONG THE HUMBER-DUNNAGE BOUNDARY ZONE, BAIE VERTE PENINSULA, NEWFOUNDLAND

R.A. Jamieson, S. Anderson, L. McDonald
Department of Earth Sciences, Dalhousie University, Halifax, Nova Scotia, Canada, B3H 3J5

L.B. Goodwin
Department of Geoscience, New Mexico Institute of Mining and Technology, Socorro, New Mexico, USA, 87801

The Baie Verte Line (BVL) of northwestern Newfoundland is a complex fault zone that separates late Proterozoic - early Paleozoic continental margin rocks of the Humber Zone from accreted early Paleozoic volcanic arcs of the Dunnage Zone. Although this boundary is widely regarded as the Taconian (Ordovician) suture along which the Iapetus Ocean closed, recent structural, seismic, and geochronological evidence suggests that this interpretation requires substantial modification. Many puzzling features of the regional geology can be explained if an episode of Silurian regional extension followed initial overthrusting and was followed by Devonian transpressional deformation.

Early structures in metaclastic rocks of the Fleur de Lys Supergroup, west of the BVL, indicate southwest-directed thrusting, possibly related to the initial Late Ordovician to Early Silurian accretion of the Dunnage Zone volcanic arcs to the Humber Zone continental margin. Later dextral strike-slip fabrics in these rocks may be associated with Silurian exhumation of deep-seated metamorphic rocks, including eclogites, west of the BVL. However, present geological relationships east of the BVL are not compatible with a simple overthrusting model. The Ming's Bight Group, a continental margin deposit correlative with the Fleur de Lys Supergroup, now occurs on the "wrong" side of the BVL. Metamorphic grade is substantially lower, and cooling ages are significantly younger, than in comparable rocks west of the BVL. The Point Rousse ophiolite complex, immediately east of the BVL, is bounded by normal faults. The Flat Water Pond Group, which trends parallel to the BVL, is separated from the Silurian Burlington Granodiorite by a normal fault; coarse conglomerate in this unit contains debris from Silurian plutons and other pre-Silurian rocks in the area. The rock units now bounded by extensional faults host numerous small gold deposits, some of them associated with Silurian shear zones. Extensional structures also occur locally in the Fleur de Lys Supergroup, although their significance with respect to other structures in the area is currently unknown. These observations could be explained if an episode of Silurian extension reworked the upper part of the Humber/Dunnage thrust stack, leaving the Ming's Bight Group and Point Rousse Complex as extensional klippen east of a graben in which the Flat Water Pond Group was deposited.

However, the BVL and rocks to the east have been strongly overprinted by later strike-slip and thrust deformation. The Silurian Dunamagon Granite and its host rocks were thrust over the Ming's Bight Group from the southeast; the thrust re-works an earlier, possibly extensional, mylonite zone. The Flat Water Pond Group was strongly deformed under greenschist facies conditions, and rocks along the BVL contain predominantly sinistral strike-slip fabrics. A seismic reflection profile (Lithoprobe East L-13) shows thrusts at mid-crustal depths that appear to post-date normal faults in the upper crust. We suggest that Acadian transpressional deformation affected the region in Devonian times, further modifying already complex structural relationships. This working hypothesis awaits testing by field and analytical studies in progress.

APPENDIX E

Microprobe data (weight %)

Sample LM-92-5

Feldspar:

SiO_2	60.996	63.103	65.418	65.412
Al_2O_3	24.376	22.819	22.744	21.989
MgO	-	-	0.119	-
FeO	-	0.162	-	-
CaO	5.948	4.145	3.368	2.972
Na_2O	7.740	8.584	8.548	9.389
K_2O	0.187	0.162	-	-
NiO	-	-	-	0.142
total	99.246	98.975	100.197	99.904

Biotite:

SiO_2	37.472	36.736
TiO_2	2.238	1.953
Al_2O_3	17.069	16.512
FeO	18.053	20.394
MnO	0.417	0.432
MgO	10.148	9.383
Na_2O	0.255	0.167
K_2O	9.530	9.675
ClO	-	0.051
total	93.183	95.303

Sample LM-92-17

	K-feldspar	Plagioclase	Biotite
SiO_2	65.843	67.138	36.751
TiO_2	-	-	3.173
Al_2O_3	18.260	21.556	15.438
FeO			24.756
MnO	0.218	-	0.507
MgO	-	0.10	6.253
CaO	-	2.339	-
NaO	0.203	10.056	0.242
K_2O	16.102	0.102	9.614
BaO	0.146	0.148	-
total	100.773	101.440	96.734

Sample LM-92-20

	K-feldspar		plagio-clase	biotite			
SiO_2	65.975	65.918	68.873	36.630	35.472	36.765	35.924
TiO_2	-	-	-	2.898	3.114	2.687	1.385
Al_2O_3	18.606	18.802	20.183	16.200	15.916	16.145	16.845
FeO	0.132	-	-	25.220	24.992	25.039	22.590
MnO	-	-	-	0.717	0.647	0.495	0.454
MgO	-	-	-	4.469	3.816	4.917	7.351
CaO	-	-	0.664	-	-	-	0.106
Na_2O	0.551	0.715	10.037	0.164	0.416	0.236	0.356
K_2O	16.083	15.861	0.137	9.870	8.775	9.579	8.163
BaO	-	0.218	-	-	-	-	-
NiO	-	0.213	-	0.301	-	-	-
ClO	-	-	-	0.072	0.035	0.093	0.144
total	101.347	101.728	99.894	96.541	93.184	95.955	93.319

Sample LM-92-39

Feldspar

SiO_2	64.735	66.258	65.103	65.047	66.082	66.056
TiO_2	0.184	-	-	-	-	-
Al_2O_3	18.812	18.946	18.757	18.739	21.373	21.298
MgO	0.092	-	-	0.080	-	-
CaO	-	-	0.078	-	2.176	1.839
Na_2O	1.737	0.763	0.932	0.670	9.377	6.900
K_2O	14.411	15.764	14.606	15.638	0.172	0.087
Cr_2O_3	-	-	-	-	0.095	-
NiO	-	-	-	-	0.304	-
BaO	-	-	0.179	-	-	-
ClO	-	-	0.059	-	-	-
P_2O_5	-	-	0.248	-	-	-
total	99.972	101.731	99.963	100.174	99.579	96.179

	titanite	magnetite	biotite
SiO_2	28.526	0.177	35.913
TiO_2	29.378	0.135	2.937
Al_2O_3	3.709	0.158	15.208
FeO	2.973	91.832	25.377
MnO	-	0.196	0.262
MgO	0.272	0.100	6.224
CaO	26.361	0.064	-
Na_2O	-	0.326	0.238
K_2O	-	0.067	9.669
NiO	-	0.301	-
P_2O_5	0.575	-	-
total	91.794	93.856	95.828

Sample LM-92-40

	biotite			titanite	feldspar		
SiO_2	36.537	35.354	35.832	29.852	65.381	65.816	61.285
TiO_2	2.448	2.608	3.254	29.961	-	-	-
Al_2O_3	15.836	15.100	16.009	5.401	18.811	21.445	17.536
FeO	23.606	24.054	23.405	1.843	-	0.366	-
MnO	0.560	0.439	0.581	0.130	-	-	-
MgO	0.726	6.818	5.915	0.101	-	-	0.075
CaO	-	-	-	27.200	-	2.117	-
Na_2O	0.201	0.290	0.338	0.132	0.844	9.404	0.589
K_2O	9.359	9.592	9.441	-	15.439	0.126	14.540
ClO	0.064	-	-	-	0.032	-	-
SrO	-	0.282	-	0.377	-	-	-
BaO	-	-	-	-	0.167	-	0.195
Cr_2O_3	-	-	-	-	-	-	0.090
total	95.335	94.537	94.774	94.997	100.674	99.274	94.311

Zoned allanite (all analyses from the same grain)

SiO_2	26.613	23.213	21.891	22.400
TiO_2	0.427	1.829	1.993	3.103
Al_2O_3	9.891	10.802	11.349	11.909
FeO	14.664	16.654	14.558	18.536
MgO	0.709	0.511	0.594	0.606
CaO	9.271	6.789	6.628	6.918
Na2O	-	0.284	0.720	1.507
ClO	0.466	0.158	0.505	0.494
SrO	-	-	-	1.008
P_2O_2	-	1.642	2.484	3.020
BaO	0.580	-	-	-
total	62.622	62.398	61.441	70.350

Sample LM-92-41

epidote

SiO_2	38.391	38.520	38.256	37.964	38.288	38.546
TiO_2	0.201	0.565	-	-	0.211	0.127
Al_2O_3	24.428	26.290	24.087	24.328	24.098	24.410
FeO	10.968	8.155	11.383	10.529	11.363	10.671
MnO	0.265	0.135	-	0.363	0.107	0.214
MgO	0.114	-	-	0.082	0.111	0.187
CaO	23.603	24.061	24.015	23.367	23.944	23.765
Na_2O	0.072	0.118	0.082	-	0.078	0.140
Cr_2O_3	-	-	0.156	-	-	-
NiO	-	-	0.181	-	-	-
total	98.043	97.844	98.160	96.633	98.201	98.061

titanite

SiO_2	30.652	30.699	30.576	30.966	30.907
TiO_2	36.300	35.944	32.325	31.855	32.065
Al_2O_3	1.926	1.604	4.259	4.216	4.152
FeO	0.475	1.136	1.310	1.290	1.006
MnO	0.141	-	-	-	-
MgO	-	-	-	0.166	-
CaO	28.586	28.512	29.397	28.865	28.844
Na_2O	0.145	-	-	0.088	-
K_2O	0.048		-	-	-
Cr_2O_3	-	0.112	-	-	0.194
ClO	-	-	-	0.098	-
NiO	0.146	-	-	0.270	0.214
BaO	-	-	-	0.764	-
total	98.329	98.007	97.867	98.573	97.383

amphibole

SiO_2	42.964	43.718	43.515	43.645	43.205	43.660
TiO_2	0.329	0.404	0.309	0.383	0.386	0.302
Al_2O_3	10.949	10.637	10.658	10.707	10.653	10.833
FeO	17.343	17.579	17.757	17.741	17.371	17.229
MnO	0.629	0.504	0.552	0.495	0.632	0.594
MgO	10.310	10.497	10.563	10.236	10.480	10.526
CaO	11.757	11.730	11.853	11.833	11.714	11.742
Na_2O	1.616	1.656	1.558	1.672	1.604	1.608
K_2O	1.527	1.512	1.484	1.565	1.526	1.495
Cr_2O_3	0.126	-	0.186	-	-	-
NiO	-	-	-	-	0.165	0.162
total	97.551	98.236	98.436	98.277	97.736	98.151

biotite

SiO2	38.533	38.919	38.923	67.574	38.524	38.889
TiO2	1.076	1.038	0.984	0.956	1.153	1.187
Al2O3	14.068	13.993	14.167	13.690	14.008	14.247
FeO	16.313	16.921	17.057	16.010	17.028	16.518
MnO	0.309	0.507	0.479	0.242	0.391	0.440
MgO	14.719	14.681	14.599	14.595	14.510	14.221
NaO	0.159	0.306	0.287	0.228	0.236	0.269
K2O	9.740	9.568	9.659	9.219	9.688	9.771
ClO	0.049	-	0.214	0.106	-	0.041
total	94.966	95.934	96.368	92.619	95.537	95.584

plagioclase

SIO_2	64.411	63.686	64.261	64.344	64.001	64.290	64.471
TiO_2	0.140	-	-	-	-	0.126	-
Al_2O_3	23.524	23.938	23.093	23.375	23.084	23.373	23.368
FeO	0.256	0.218	-	0.335	0.154	0.295	0.110
MnO	-	-	-	-	-	-	0.100
CaO	4.372	4.752	4.184	4.009	4.306	4.446	4.307
Na_2O	8.428	8.946	8.420	7.555	8.671	8.830	8.223
K_2O	0.218	0.209	0.307	0.255	0.195	0.165	0.204
NiO	0.261	0.148	-	-	-	0.158	0.158
BaO	-	0.197	-	-	-	-	0.153
Cr_2O_3	-	0.079	-	-	-	-	-
total	101.610	102.172	100.255	98.872	100.41	101.684	101.095

K-feldspar

SiO_2	65.907	65.826	65.211
Al_2O_3	18.812	18.745	18.689
MgO	0.089	0.082	-
Na_2O	0.929	1.029	1.138
K_2O	14.985	15.929	15.178
ClO	0.183	-	-
BaO	-	0.159	0.287
NiO	-	-	0.142
total	100.905	101.770	100.645

Sample LM-92-46

amphibole

SiO_2	41.494	40.781	40.553	41.201	43.457	40.988	43.771	43.610
TiO_2	0.602	0.615	0.557	0.455	0.536	0.498	0.520	0.389
Al_2O_3	14.919	14.877	14.648	14.303	11.696	14.330	11.358	11.429
FeO	20.740	20.368	19.812	19.979	19.178	20.464	19.081	18.992
MnO	0.206	0.352	0.435	0.447	0.464	0.592	0.453	0.391
MgO	7.157	7.039	6.861	6.942	8.586	7.059	8.728	8.725
CaO	12.100	11.892	11.623	11.906	11.951	11.837	11.798	11.543
Na_2O	1.412	1.367	1.355	1.303	1.301	1.405	1.136	1.129
K_2O	1.211	1.144	1.183	1.076	0.951	1.103	0.934	0.874
Cr_2O_3	0.180	-	0.105	-	-	-	-	-
NiO	0.170	-	-	-	0.207	0.174	-	-
ClO	0.202	0.191	0.287	0.172	-	0.209	-	-
total	100.415	98.626	97.419	97.784	98.326	98.659	97.778	97.082

feldspar

SiO_2	60.788	61.266	66.587	62.975	63.139	67.093
TiO_2	-	-	-	-	24.651	0.091
Al_2O_3	25.030	24.803	22.421	24.313	0.663	21.714
FeO	0.116	0.295	-	0.283	-	-
MnO	-	-	-	-	0.092	
MgO	-	-	-	0.207	-	0.082
CaO	6.355	5.543	200	1.236	5.302	2.127
Na_2O	7.290	6.447	6.059	5.974	7.477	6.065
K_2O	0.185	0.411	0.413	2.583	-	0.101
Cr_2O_3	0.101	-	-	-	-	-
BaO	-	-	-	0.149	-	-
NiO	0.137	0.147	-	0.231	-	-
ClO	-	0.057	0.119	-	0.047	0.422
total	100.002	98.968	97.600	97.951	101.371	97.686

	epidote			opaque	carbonate
SiO_2	42.159	38.313	38.190	1.870	0.156
TiO_2	0.094	0.540	-	-	-
Al_2O_3	24.766	26.721	26.395	-	0.099
FeO	1.083	7.761	8.701	77.171	0.351
MnO	0.169	0.097	0.132	-	0.399
MgO	0.377	0.103	-	-	0.135
CaO	24.756	23.928	23.697	-	55.779
Na_2O	-	0.146	0.100	0.440	-
Cr_2O_3	-	-	0.123	-	-
NiO	-	-	0.155	0.478	0.202
ClO	-	-	0.036	-	-
BaO	-	0.212	0.160	-	-
ZrO_2	-	0.169	-	-	-
SrO	-	-	-	4.572	-
P_2O_5	-	-	-	-	0.126
Nb_2O_5	-	-	-	-	0.176
total	93.404	97.989	97.688	84.531	57.422

Sample LM-92-51

titanite

SiO_2	32.524	29.563	30.131	29.233	29.587	30.653	28.882
TiO_2	28.879	31.364	31.696	30.222	31.224	33.602	30.378
Al_2O_3	3.777	4.492	4.261	4.472	4.304	3.733	3.365
FeO	1.503	1.597	1.465	1.495	1.371	1.159	1.383
MnO	-	-	0.163	0.122	0.146	0.153	0.110
MgO	3.062	-	0.101	0.150	-	0.066	0.078
CaO	24.793	26.223	27.376	26.228	26.762	28.614	26.474
Na_2O	0.326	0.098	0.128	0.177	0.099	-	0.119
Cr_2O_3	0.101	-	-	-	-	0.137	-
NiO	0.183	0.202	-	-	-	-	-
ClO	0.246	-	0.061	0.041	-	-	-
P_2O_5	0.650	0.836	0.296	1.302	0.701	-	0.426
BaO	-	-	-	0.410	-	-	-
Nb_2O_5	-	-	-	0.829	0.939	-	1.565
total	96.042	94.375	95.679	94.683	95.133	98.117	92.778

	biotite			chlorite	apatite
SiO_2	34.628	26.163	26.468	23.535	-
TiO_2	2.424	-	-	-	0.284
Al_2O_3	16.052	19.197	20.290	20.771	0.079
FeO	23.234	33.882	29.534	35.198	0.388
MnO	-	0.492	-	0.529	-
MgO	6.333	9.593	7.754	7.509	-
CaO	-	-	0.066	-	55.704
Na_2O	0.184	0.302	0.314	0.350	0.190
K_2O	7.653	-	-	-	-
NiO	-	-	-	-	0.174
Cr_2O_3	0.086	-	-	0.112	-
P_2O_5	-	-	-	-	41.771
BaO	-	-	-	0.187	-
ZrO_2	-	-	-	-	0.675
Nb_2O_5	-	-	-	-	0.314
total	90.594	88.629	85.133	88.191	99.579

	K-feldspar porphyro-clast			exsolu-tion lamellae	plagio-clase	
SiO2	64.787	64.016	64.897	67.877	69.345	70.437
TiO2	-	-	-	0.127	-	-
Al2O3	18.811	18.234	18.675	20.333	19.782	19.756
FeO	-	-	0.145	-	-	-
MgO	0.079	-	-	-	0.469	-
CaO	-	-	-	0.856	0.328	-
Na2O	0.876	1.559	0.958	9.862	9.746	11.424
K2O	15.340	14.167	15.750	0.440	0.041	-
BaO	0.426	-	0.180	-	-	-
NiO	-	-	-	-	-	0.251
Cr2O3	0.115	-	-	-	-	-
P2O5	-	0.147	-	-	-	0.155
total	100.433	98.122	100.605	99.496	99.710	102.024

APPENDIX F

Station locations: detailed maps

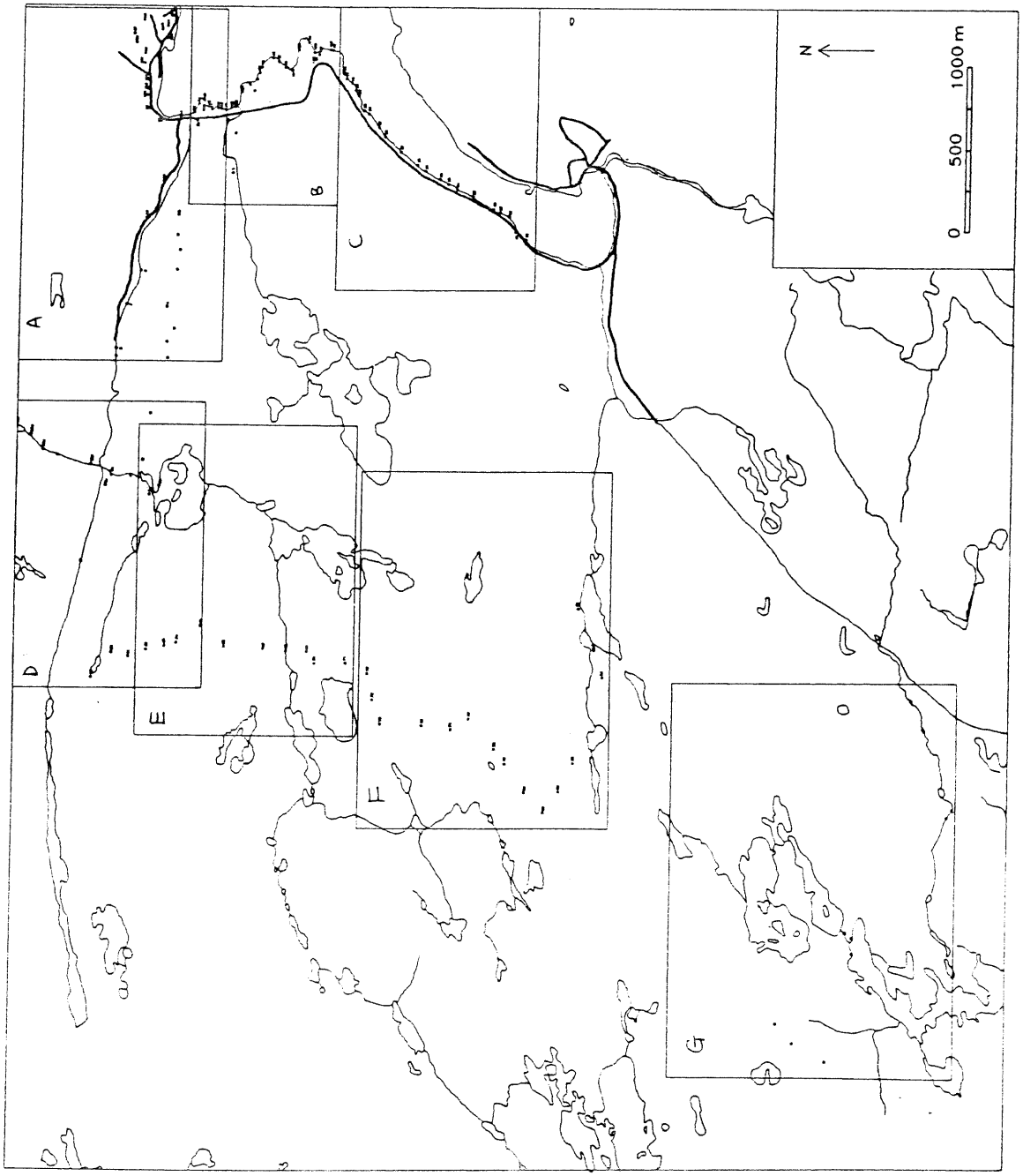

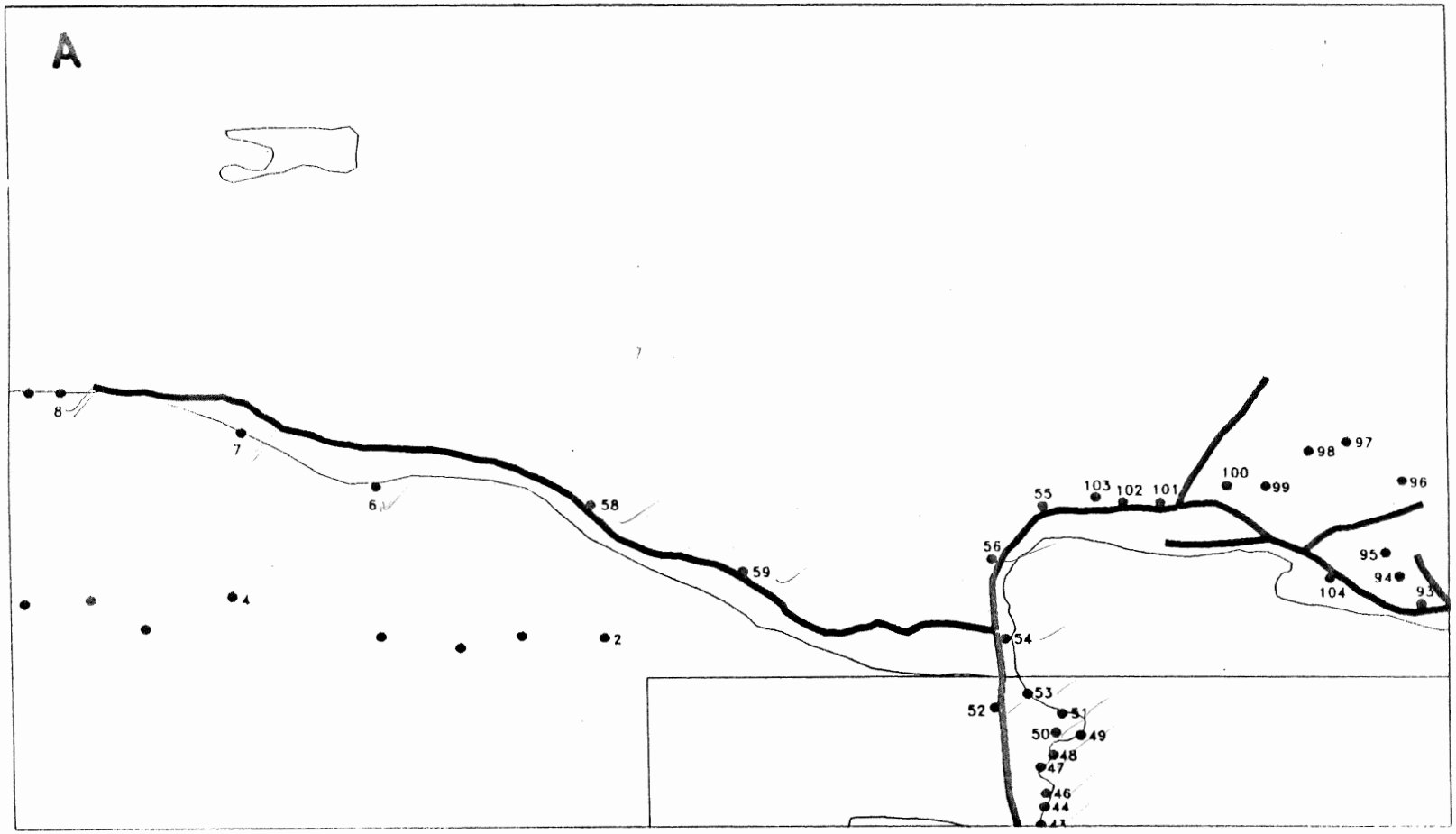
A
8
7
6
58
59
4
2
55
103
102
101
100
99
98
97
96
56
95
94
104
93
54
53
52
51
50
49
48
47
46
44
43

F2

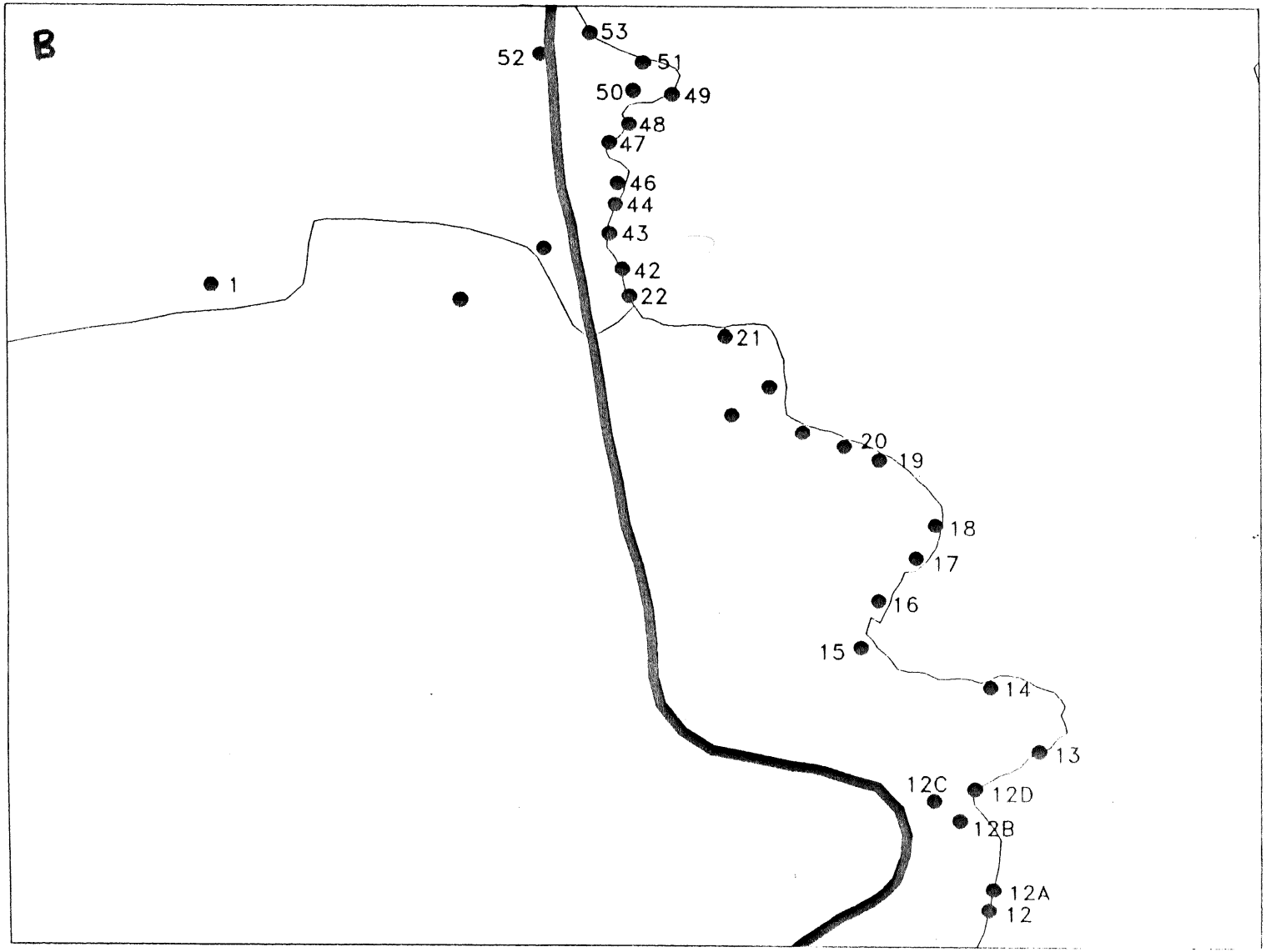
B
53
52
51
50
49
48
47
46
44
43
42
22
1
21
20
19
18
17
16
15
14
13
12C
12D
12B
12A
12

F3

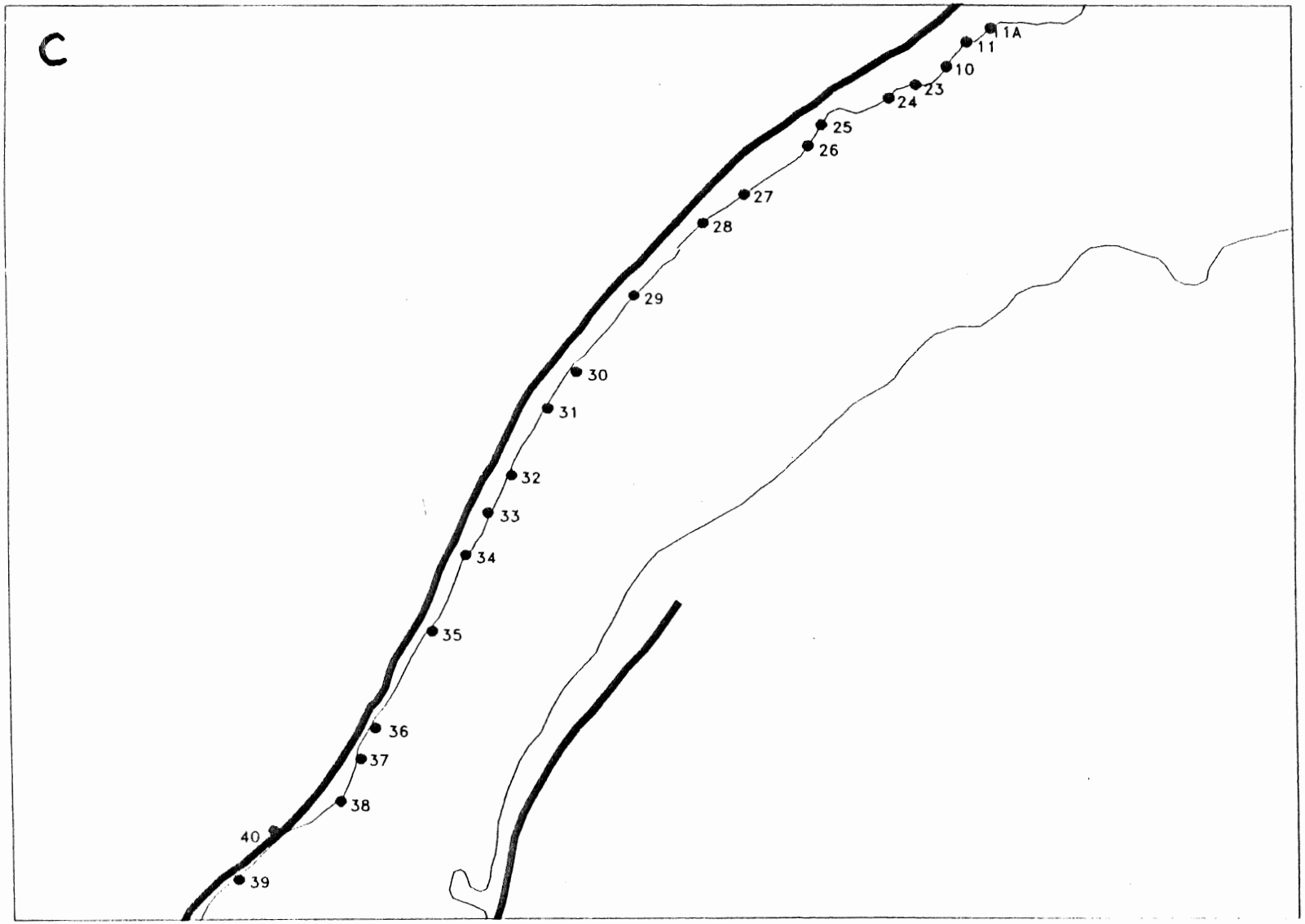

F4

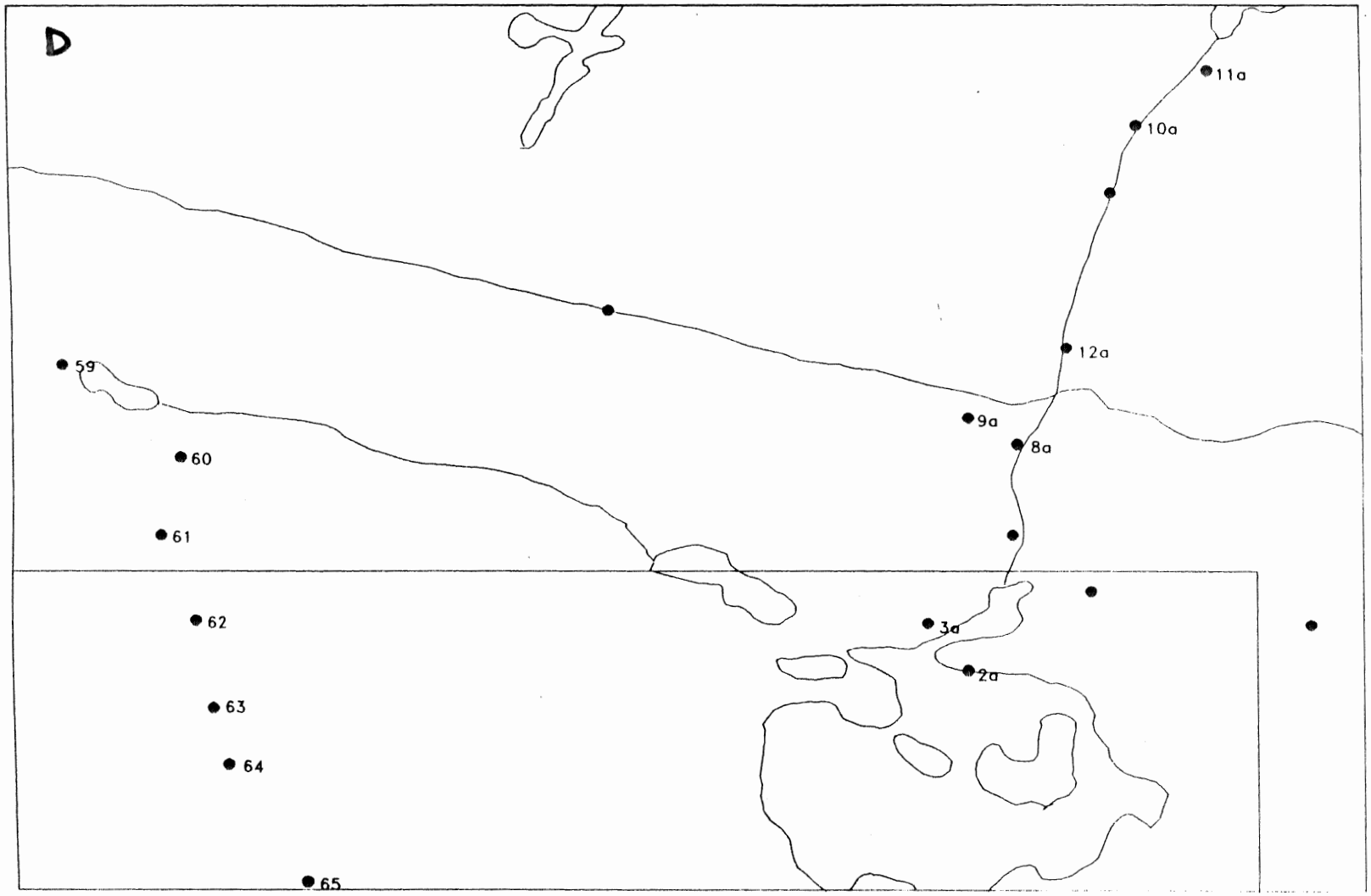

F5

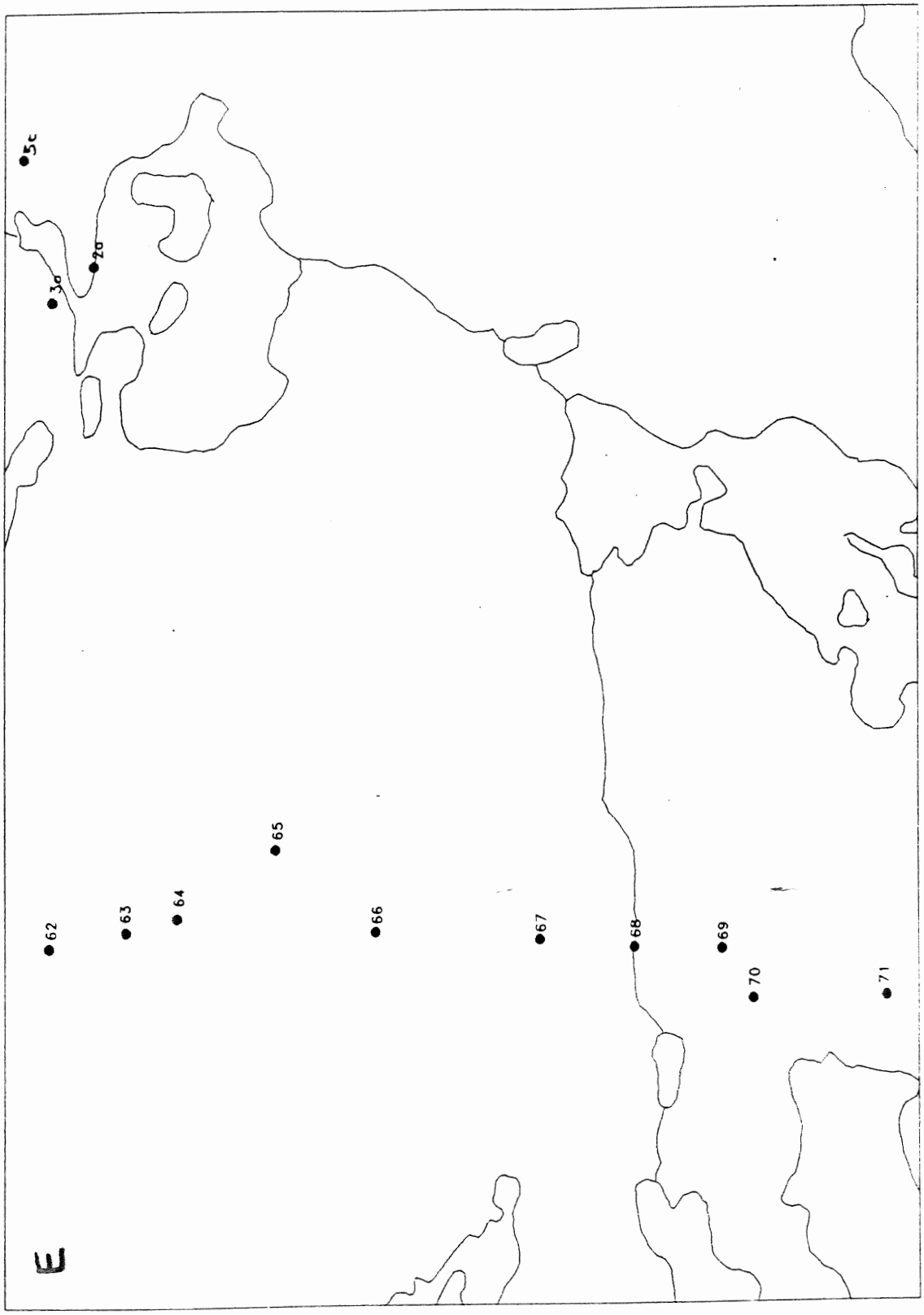
5c
2a
3a
62
63
64
65
66
67
68
69
70
71
E

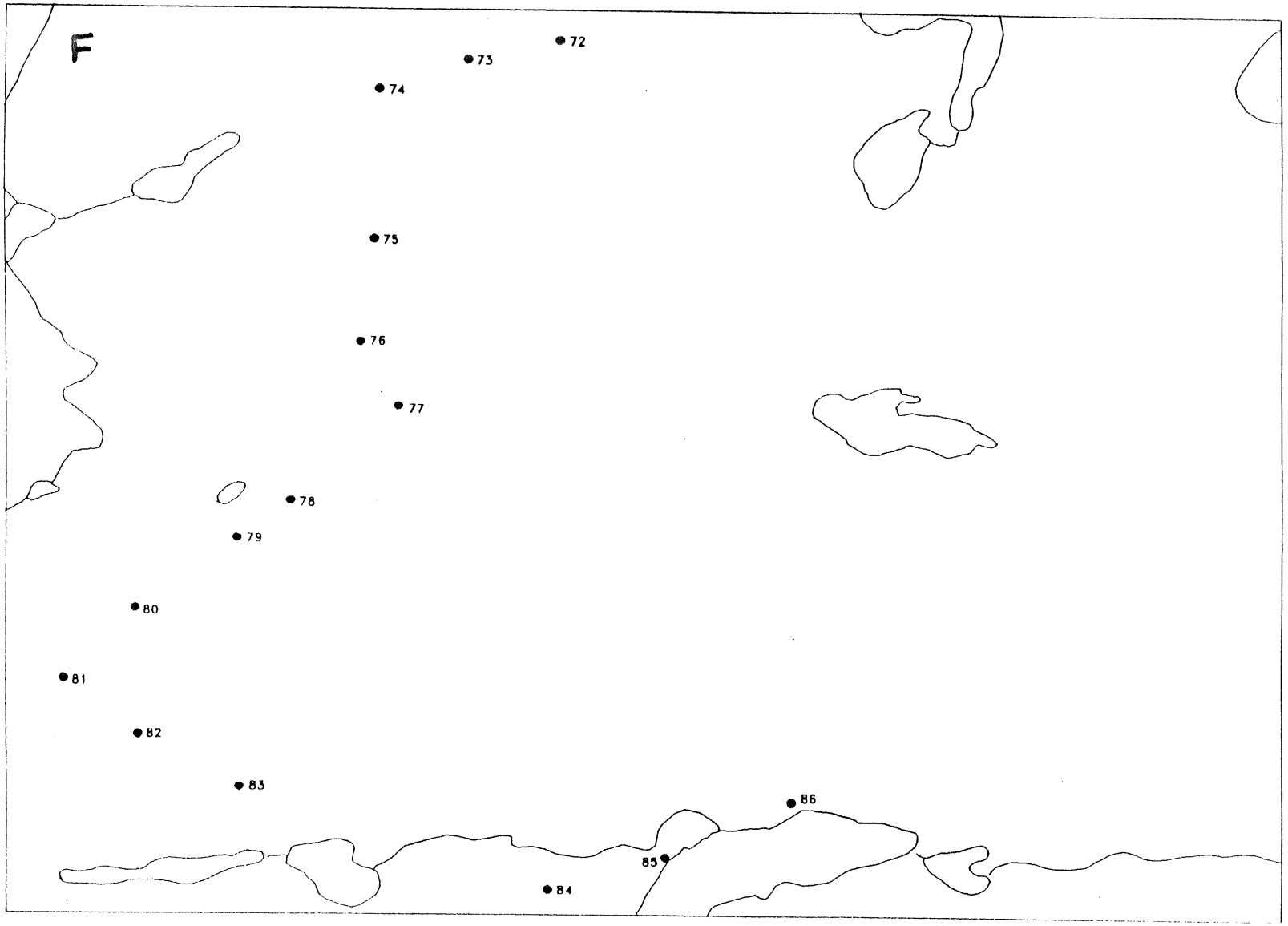

F7

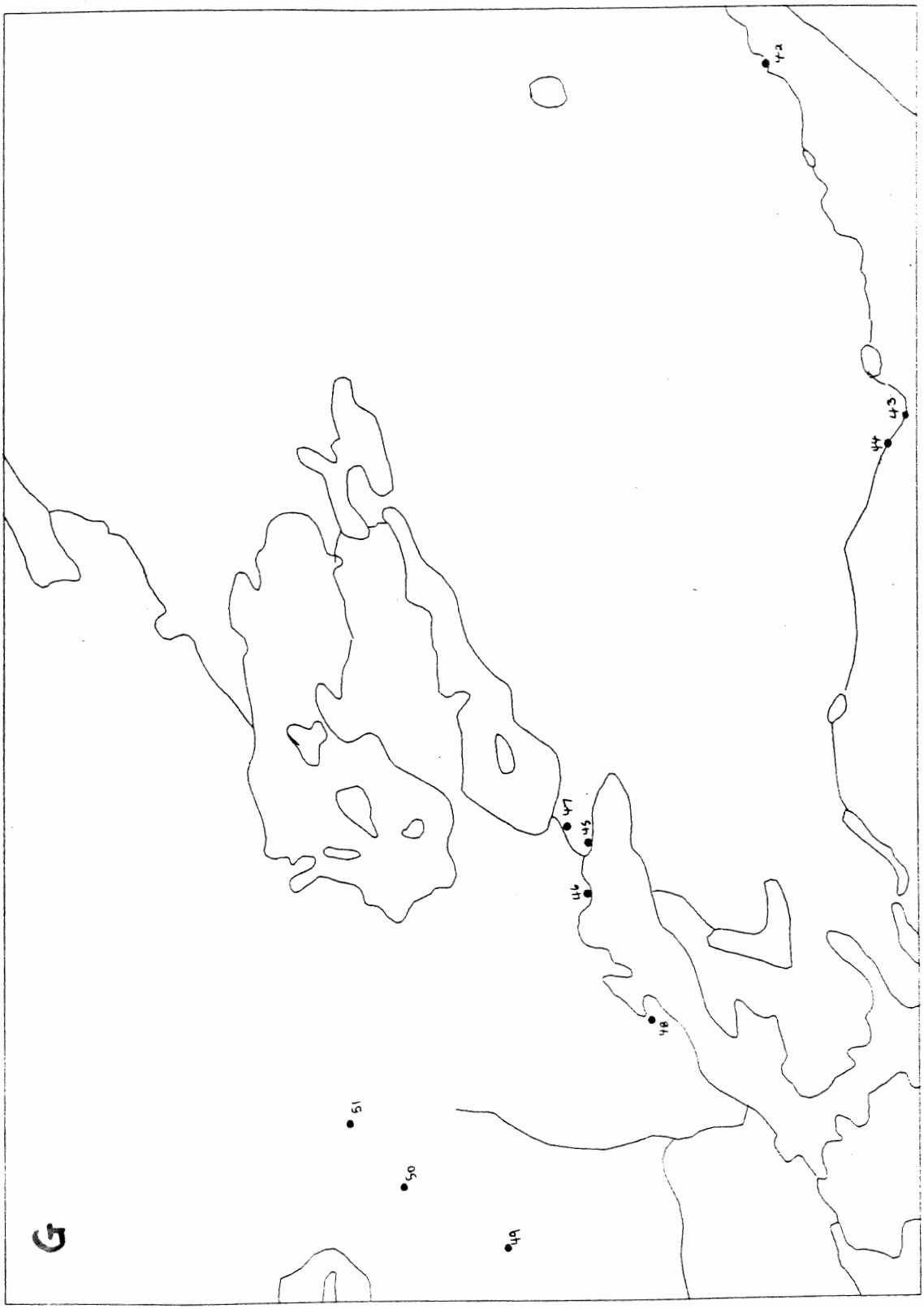
42
43
44
45
47
46
48
49
50
51
G